HydroHaptics: High-Fidelity Force-Feedback on Soft Deformable Interfaces using Hydrostatic Transmission

James Nash
University of Bath
Bath, United Kingdom
jn688@bath.ac.uk

Kim Sauvé
University of the West of England
Bristol, United Kingdom
kim.sauve@uwe.ac.uk

Catharina Maria van Riet
Eindhoven University of Technology
Eindhoven, Netherlands
AMOLF
Amsterdam, Netherlands
c.m.v.riet@tue.nl

Anke van Oosterhout
Eindhoven University of Technology
Eindhoven, Netherlands
a.v.oosterhout@tue.nl

Adwait Sharma
University of Bath
Bath, United Kingdom
as5339@bath.ac.uk

Christopher Clarke
University of Bath
Bath, United Kingdom
cjc234@bath.ac.uk

Jason Alexander
University of Bath
Bath, United Kingdom
jma73@bath.ac.uk

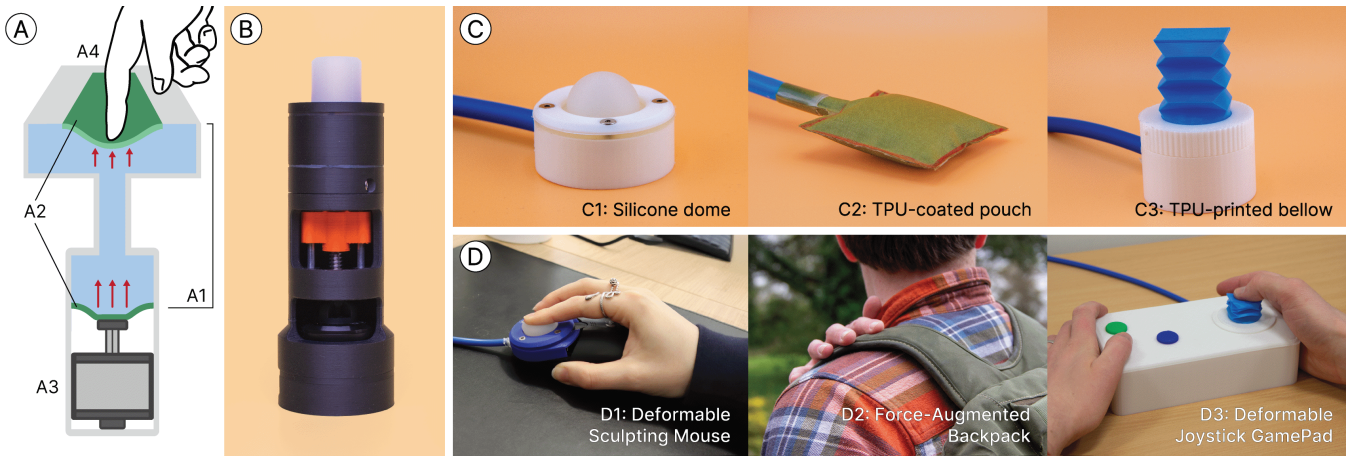

Figure 1: HydroHaptics renders detailed haptic effects onto deformable interfaces. (A) The *Hydrostatic Transmission* concept for HydroHaptics utilises a hydraulic cell (A1) which couples two flexible surfaces (A2), connecting the electromechanical haptic engine (A3) and deformable interface (A4). (B) An implementation of the HydroHaptics platform, with a silicone tube interface. We developed several compatible deformable interfaces (C), including a silicone dome (C1), TPU-coated fabric pouch (C2) and TPU-printed bellows (C3). We implement these interfaces in a range of applications (D), including a force-augmented deformable 3D sculpting mouse (D1), force-augmented backpack (D2) and a 3-axis deformable force-augmented joystick (D3).

Abstract

Soft deformable interfaces offer unique interaction potential through input flexibility and diverse forms. However, force feedback on these devices remains limited, with pneumatic approaches lacking responsiveness and precision, while microhydraulic solutions are constrained to small form factors with limited input. We present HydroHaptics, a novel platform that enables high-fidelity force feedback on deformable interfaces via hydrostatic transmission. Surpassing current state-of-the-art methods, our approach allows fine-grained force feedback on soft interfaces, achieving a 10 N force change in < 100 ms and accurate 1 N, 10 Hz oscillation rendering. We detail the system's design and implementation, highlighting its ability to maintain the inherent interaction benefits of soft interfaces. A user study ($N = 18$) evaluates the system's performance, showing high accuracy in rendering distinct haptic

UIST '25, Busan, Republic of Korea

ACM ISBN 979-8-4007-2037-6/25/09
https://doi.org/10.1145/3746059.3747679

effects (82.6% accuracy) and classifying input gestures (89.1% accuracy). To showcase the platform's versatility, we present four applications illustrating HydroHaptics' potential to enhance interaction with deformable devices and unlock novel user experiences.

CCS Concepts

• **Human-centered computing → Haptic devices**; **Interaction devices**.

Keywords

Deformable interfaces, Haptics, Non-rigid interactions, Tangible Interactions, Force Feedback

ACM Reference Format:

James Nash, Kim Sauvé, Catharina Maria van Riet, Anke van Oosterhout, Adwait Sharma, Christopher Clarke, and Jason Alexander. 2025. HydroHaptics: High-Fidelity Force-Feedback on Soft Deformable Interfaces using Hydrostatic Transmission. In *The 38th Annual ACM Symposium on User Interface Software and Technology (UIST '25), September 28–October 01, 2025, Busan, Republic of Korea.* ACM, New York, NY, USA, 20 pages. https://doi.org/10.1145/3746059.3747679

1 Introduction

We present HydroHaptics, a novel system capable of significantly enhancing the quality of dynamically adjustable force feedback on soft, compliant interfaces, while preserving their inherent softness, flexibility in form, and freedom of input—qualities that enable rich and novel user experiences. HydroHaptics utilises a fixed volume of liquid within a sealed ***Hydraulic Cell*** (Figure 1A, A1) which has two flexible surfaces (A2). Since the enclosed liquid is incompressible, it hydraulically couples the two surfaces, enabling bi-directional force transmission between them. The ***Haptic Engine*** (A3)—a linear mechanical actuator—can dynamically provide force feedback by displacing the fluid in the hydraulic cell, transmitting force to the ***Deformable Interface*** (A4). Similarly, to allow the interface to deform, the Haptic Engine moves in response to the force applied to the Deformable Interface, maintaining the pressure within the hydraulic cell, which can be adjusted to render different stiffness levels to the user. This approach can be used to render sharp clicks [46, 120], oscillating forces [11, 17], and dynamic resistance or input halting [30]. Simultaneously, input from the user can be sensed by monitoring the internal pressure. As a result, HydroHaptics enables unique haptic experiences on soft, deformable interfaces—such as dynamic simulations for medical training or providing sharp tactile notifications on soft wearables—which are impractical using current approaches.

Previous approaches have used pneumatics to provide force feedback on deformable devices due to its high force output range [88], compatibility with diverse form factors [99, 113], and relative affordability and availability of components [61]. However, the compressibility of air limits the accuracy and speed of force and displacement output [88]. In contrast, hydraulic systems use liquid—with negligible compressibility—as the working fluid, allowing for greater precision and more responsive output. Currently, interactive hydraulic systems primarily utilise microhydraulics [10, 18, 73], which leverage this increased control but, due to volume limitations, constrain the interface to small buttons mounted on rigid surfaces [72]. This sacrifices the input flexibility and diversity of forms that enable the rich interaction potential of deformable devices. Furthermore, designing hydraulic interactive systems is non-trivial due to leakage, limited back-drivability, and the reliance on specialised components [88].

HydroHaptics has several advantages over previous fluid-based deformable force-feedback systems. First, unlike traditional pneumatic or hydraulic systems that require pumps, valves, and regulators, HydroHaptics is powered by a brushless DC motor, leveraging their affordability, availability, and control options [75]. This enables us to extend the haptic authoring tool "Feelix" [94] to support the creation of force-feedback effects on HydroHaptics. Second, it is designed to be robust and scalable, with fewer components, reducing susceptibility to leaks and making the system adaptable to larger interfaces. Third, the concept underpinning HydroHaptics is inherently bi-directional, which enables sensing of force input interactions simultaneously with force feedback. In sum, this provides unique opportunities for designers and researchers to explore haptic interactions on soft interfaces and develop novel deformable devices, enabling future research.

We evaluated the performance of HydroHaptics through a series of technical evaluations using a high-precision robot arm, followed by a user study ($N = 18$). Evaluations of HydroHaptics under stationary conditions—in which system pressure remained static—demonstrated high accuracy in sensing internal pressure ($\sigma = 0.23\ kPa$) and in estimating input displacement ($\sigma = 0.18\ mm$) and force ($\sigma = 0.17\ N$). Dynamic tests—with time-varying pressure—highlighted the system's responsiveness, surpassing the force feedback capabilities of previous deformable interfaces. HydroHaptics achieved rapid pressure changes of 30 kPa (20 N) in under 100 ms and near-lossless rendering of a 10 Hz, 2 N sine wave. During the user study, HydroHaptics' ability to create distinct haptic effects—such as *clicks*, *button* and *oscillation*—was demonstrated, with an average identification accuracy of 82.6% across all effects and 92.8% on the most distinct effect. Furthermore, data collected from HydroHaptics while participants' performance input gestures enabled classification-based recognition, achieving an average user-dependent accuracy of 89.1% demonstrating its ability to recognise deformable gestures.

HydroHaptics explores the potential of high-fidelity dynamic force feedback on deformable devices. We developed several applications to demonstrate how HydroHaptics enhances interaction through fine-grain force feedback. These applications include a force-augmented mouse that supports deformation inputs with tactile confirmation and continuous feedback (Figure 1, D1), an interactive cushion that delivers haptic feedback such as clicks and vibrations while maintaining its softness, a backpack that provides on-body force feedback through the straps to offer directional cues and notifications via taps and presses (Figure 1, D2), and a 3D-printed force-augmented joystick that enhances video game immersion by delivering 'push-off' feedback to the user (Figure 1, D3).

To summarise, this paper makes the following contributions: (1) The working concept of HydroHaptics along with the system design, describing how it was designed to align with user and designer goals. (2) The design and fabrication of HydroHaptics, including 3D models and platform code to support replication and adaptation, along with an updated version of the "Feelix" haptic authoring

tool for creating force-feedback effects [58]. (3) Technical and user evaluations of the force-feedback and input sensing capabilities of HydroHaptics. (4) Four applications for the HydroHaptics platform, highlighting its potential to deliver detailed haptics on deformable interfaces.

2 Related Work

2.1 Deformable Devices

Compliant devices—capable of moving or changing shape in response to applied force—encompass a range of input mechanisms, including buttons [46], sliders [40], dials [95, 97], and pin arrays [20, 54]. Compliant devices can be divided into two categories [7, 57, 77]: which we term, *Movable* and *Deformable*. Movable devices such as "HapticLever" [21], "FlexHaptics" [47] and "Mantis" [5], consist of rigid, articulated components, such as links and rods, that reconfigure or move relative to one another. Their predefined movement paths allow for controlled actuation, creating changes in overall shape without the deformation of individual parts. In contrast, deformable devices are made from soft, elastic, or malleable materials, enabling direct physical deformation by the user.

This fundamental difference in construction significantly influences the user experience. First, the malleability of deformable devices expands the input degrees-of-freedom, enabling a broad range of gestures, including pinching [63], shearing [102], twisting [33, 39], bending [16, 24], and squeezing [98]. Second, as deformable devices do not require rigid mechanisms to achieve compliance, the range of possible interface shapes is much greater. This is highlighted in the diverse range of geometries of existing deformable devices, including replicating everyday objects [69, 71], organic [53] and irregular [62] shapes, and wearables [65]. Finally, deformable devices can be constructed with no rigid parts or hard edges [56, 69, 76, 98] and can be integrated into existing soft objects without degrading the users' comfort. This makes them ideal for objects such as pillows [9], cushions [98], car seats [4] or wearable items [63], where movable devices, with rigid elements, would be unsuitable.

These advantages highlight the impact of deformable devices in HCI. The increased input potential, device freedom-of-form, and inherent softness enable designers to create interaction experiences that are radically different from those with movable devices.

2.2 Force Feedback on Deformable Devices

Force feedback naturally lends itself to compliant devices, and prior work has explored its potential uses on deformable devices [36, 54, 74, 120]. Medical simulation devices leverage the compliance of deformable interfaces to enhance realism [91]. Soft wearables have integrated force feedback to provide tactile experiences, such as squeezing the wrist [65] or applying pressure to the torso [14]. Researchers have also studied the role of stiffness in input performance [22] and its effects on user perceptions and associations [80, 82]. Additionally, pneumatic systems with multiple chambers can replicate the complexity of everyday soft objects [51, 114].

However, in current implementations, even across different actuation methods, there is a tradeoff between achieving dynamic, accurate and responsive force feedback, and preserving the benefits of deformable devices. Granular jamming [19, 78] enables rapid switching between discrete stiffness levels but cannot render intermediate values. Smart materials, such as MR fluids [35] and hydrogels [52, 81], have also been used, though these are often supported by rigid structures, limiting overall deformability. Passive approaches, like "FabriClic" [27] and "SnapInflatables" [112], employ multiple stable states to provide tactile click-like feedback, but their discrete nature and form-factor constraints limit versatility.

Pneumatic actuation is widely used in deformable devices [11, 13, 25, 31, 59, 65, 113, 117], with force-feedback characterisation conducted on some pneumatic devices. "ForceJacket" [14] utilised pneumatic airbags for force feedback but demonstrated limited performance, with a response time of 0.8 s (1.25 Hz) when switching between 1.5 N and 5.5 N. "PneuSleeve" [121] used pneumatic compression actuators and demonstrated an improved response time of 0.3 s, though within a smaller range (0.2 N to 1.3 N). The device also exhibited a 75 % drop in force magnitude between 1 Hz and 10 Hz, highlighting the limitations of pneumatic systems due to air compressibility. In contrast, "JetUnit" [119], a hydraulic system, showed only a one-third reduction in force output at 10 Hz, demonstrating the potential of hydraulic systems to provide enhanced haptic experiences, as explored in the next section.

Augmented deformable devices with force feedback enable novel interaction experiences. However, their potential uses are restricted by their limited responsiveness and precision. Improvements to performance could open up new devices and applications.

2.3 Hydraulically-driven Haptics

There are two main approaches for the use of hydraulics in haptics The first uses mechanical pumps to drive fluid through the system, enabling significantly higher flow rates but requiring larger, bulkier hardware. For example, "HydroRing" [29] uses peristaltic pumps to deliver water at varying temperatures, while "JetUnit" [119] leverages high-pressure water to create on-body haptic experiences. The second approach involves "micro-hydraulics", using micropumps such as electroosmotic [66, 73], electrohydrodynamic [23], or HASEL (Hydraulically Amplified Self-Healing Electrostatic) actuators [10]. These systems achieve exceptionally high flow rates relative to their size but are challenging to scale up, as they are typically limited to flow rates of less than 10 millilitres per minute [73]. While ideal for small-scale applications such as on-finger devices [72], they are not currently suitable for rapid actuation of volumes over 0.1 ml.

HydroHaptics uses a mechanical actuator to push a fixed fluid volume. A similar approach was used in "Hydrauio" [109] and Youn et al. [115] utilised hydraulic coupling in *"HaptiCoil"*, to transfer high-frequency oscillations from a micro-speaker to a user's fingertip. This approach offers the potential to render detailed force feedback on larger volume systems while avoiding the need for mechanical pumps.

3 HydroHaptics Design

The HydroHaptics concept (Figure 1A) uses mechanical actuation to produce haptic effects through a hydraulic cell. This section

describes how we translated this concept into the HydroHaptics platform, considering the perspectives of both users and designers.

3.1 Design Goals

To guide the design, we defined two sets of goals: User-Centred (UC), focusing on the user experience, and Design-Centred (DC), for the needs of designers or researchers deploying the system. These goals were informed by the authors' existing expertise in conjunction with knowledge from related work:

- **UC1** Enable fine-grained, dynamic force feedback—*This draws on existing haptic force feedback devices and their granularity [30, 97, 120].*
- **UC2** Compatible with a wide range of deformable interfaces.
- **UC3** Facilitate diverse and creative deformable inputs.

***UC2** and **UC3** stem from the benefits of deformable interfaces (outlined in subsection 2.1), as discussed in "Non-Rigid HCI" [7].*

- **DC1** Avoid reliance on specialised components or parts—*reflecting concerns about toolkits requiring specialised equipment or software, as discussed by Ledo et al. [42].*
- **DC2** Robust and leak-proof design—*arising from technical challenges with hydraulic shape-changing devices [88].*
- **DC3** Enable the authoring of haptic effects—*this builds on prior work in enabling user-authored haptic effects [47, 94, 119].*

These design goals informed the process of developing the final implementation of HydroHaptics. We indicate where specific goals shaped particular choices, offering insight into the rationale behind the design process.

3.2 Design Overview

As shown in Figure 2, HydroHaptics comprises a **haptic engine**, connected to the **deformable interface** via the **hydraulic cell**. The haptic engine and the deformable interfaces are hydraulically coupled by the liquid (water) sealed inside the system, which transmits force and motion. By controlling and measuring the fluid displacement within the haptic engine, HydroHaptics can vary the stiffness profile of the deformable interface, and detect user inputs.

3.3 Haptic Engine

The Haptic Engine (Figure 2) provides linear mechanical force and position input to control the pressure within the hydraulic cell, generating and regulating force feedback. Selecting an appropriate actuator for the Haptic Engine is key to achieving the required haptic capabilities. We chose a Brushless DC (BLDC) motor for HydroHaptics for two key reasons. First, BLDC motors are affordable, reliable, and readily available in diverse configurations, and are widely used across various applications (e.g. drones, power tools, and e-bikes) [**DC1**]. Second, BLDC motor torque and speed can be precisely controlled using field-oriented control (FOC) and robust, off-the-shelf open-source tools such as "SimpleFOC" [75] [**UC1**, **DC3**]. Consequently, BLDC motors are well suited for interactive devices such as *"Feelix"* [94], "SmartKnob" [6], and "TorqueCapsules" [111]. A lead nut mounted on the motor can drive a lead screw to convert the rotational output of the BLDC motor to linear movement. As a result, our approach uses low-cost, off-the-shelf components to create a low-friction transmission, minimising losses from the motor [**DC1**].

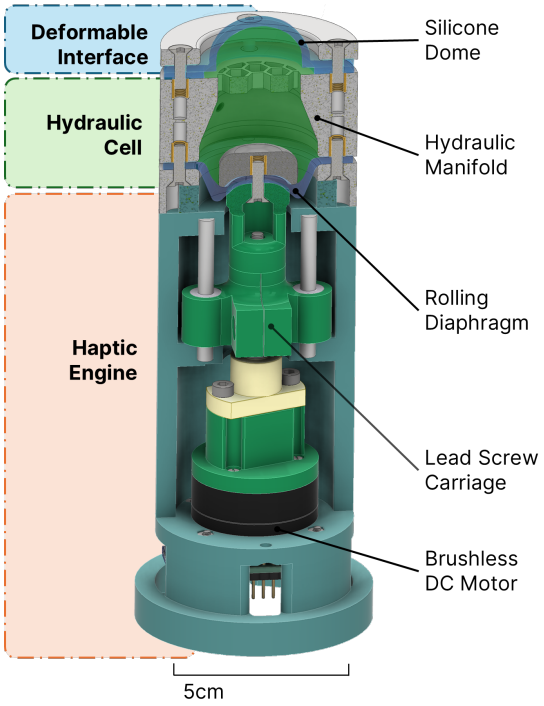

Figure 2: An overview of an implementation of HydroHaptics platform. The Haptic Engine is connected to the Hydraulic Cell via the Rolling Diagram. The hydraulic cell couples the haptic engine's force output to the deformable interface.

There is a wide variety of BLDC motors available, ranging in performance, size and price. Higher-power BLDC motors can provide increased torque and speed output, enabling increased **force precision**, wider **force range** and faster **interaction speed**. However, they are more expensive, larger in size, and generate significant heat, which requires proper dissipation to prevent performance issues or safety risks.

3.4 Hydraulic Cell

The Hydraulic Cell (Figure 2) encloses the working fluid and needs to be robust and leak resistant throughout the pressure range [**DC2**] while avoiding reliance on specialised components [**DC1**]. The hydraulic cell can be extended with generic pneumatic tubing and fittings, both to locate the deformable interface away from the haptic engine and to connect pressure sensors for control and input sensing [**DC1**]. To minimise distortions in force output, we required a working fluid with a high bulk modulus—to limit compression—and low viscosity—to reduce flow resistance. While various fluids could be used within the hydraulic cell, water was selected as it offers both of these properties. Although other fluids such as mercury and acetone exceed water in one of these aspects, they are impractical due to factors such as toxicity, volatility, and handling difficulty. Similarly, hydraulic fluid has some advantageous properties, but brings with it significant risks to thoses using the system [34]. In

contrast, water is readily available, safe to handle, and environmentally friendly.

3.5 Rolling Diaphragm

The rolling diaphragm (Figure 3) is the flexible interface through which the haptic engine can act on the cell's liquid. As the haptic engine moves downwards the walls of the rolling diaphragm "roll" (Figure 3A-D), creating space within the hydraulic cell for fluid to flow into, allowing the user to compress the deformable interface. This must remain leak-proof throughout the haptic engine's full range of motion without restricting its movement. We moulded the rolling diaphragm from silicone, with custom moulds created to allow for the dimensions to be adapted as necessary [**DC1**]. We opted against conventional hydraulic or pneumatic cylinders, as their reliance on internal seals can introduce additional friction, causing sticking and jumping, which could disrupt force feedback control. They are also prone to leakage and air ingress, compromising reliability. In contrast, rolling diaphragms provide a low-friction, leak-proof alternative by unrolling smoothly under force [107] [**DC2**].

3.6 Deformable Interfaces

Facilitating deformable interaction [**UC3**] on a diverse range of deformable interfaces [**UC2**] is a core aim of HydroHaptics. The deformable interface must be compliant while remaining airtight and leak-proof [**DC3**]. It should also be practical to fabricate in various forms and sizes. Selecting a single type of deformable interface that would enable a diverse and varied range of potential interfaces and interactions is impractical. Instead, we opted for three different interface types, which have distinct benefits and drawbacks that make them well-suited to specific applications. The three input types we explored were:

3.6.1 Cast Silicone. Silicone interfaces (Figure 5A) are elastic, soft, resilient, and waterproof **[DC2]** and can be cast into a wide range of shapes and stiffnesses. Their flexibility allows users to twist, pull, and squash them with minimal restriction **[UC3]**. Although softer interfaces are more prone to deformation from internal pressure [118]. The fabrication of silicone parts requires some specialised equipment, particularly a degassing chamber, to achieve defect-free parts. There are also limitations to the forms that can be cast. Creating internal cavities is particularly difficult, either requiring complex multi-part moulds, creating separate parts to be bonded after curing or the use of sacrificial inner moulds [59].

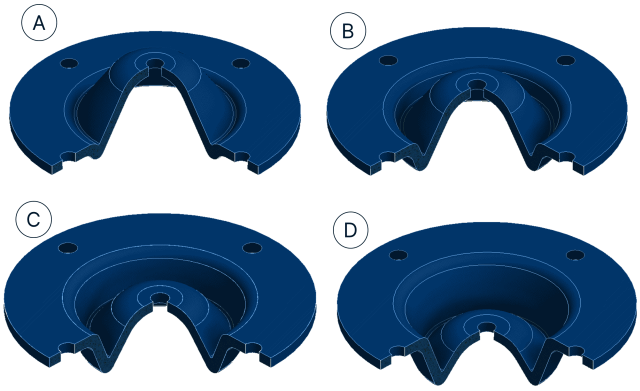

Figure 3: A 3D rendering of the rolling diaphragm which transmits force through the hydraulic cell in four different positions, going from highest (A) to lowest (D). These positions are changed by the haptic engine acting upon the centre of the diaphragm.

3.6.2 3D-printed TPU. 3D printing TPU (Figure 5B) is an increasingly prevalent method for fabricating elastic parts. Offering an approach to creating unique complex interfaces that would be difficult or impossible to achieve through casting. Furthermore, TPU-compatible 3D printers are common in most research and design labs **[DC1]**, enabling parts to be created in a single automated process. This approach still has some limitations. The range of available shore hardnesses is limited—ranging from 40D to 60A shore hardness, and some shapes are not possible on commercial 3D printers. Additionally, it remains challenging to produce robust, airtight, thin-walled structures [79, 116].

3.6.3 Heat-sealed TPU. The final method uses sheets of Thermoplastic Polyurethane (TPU), heat-bonded together to form sealed pouches, enabling the rapid production of deformable interfaces (Figure 5C). This method supports the creation of large pouches with internal cavities—geometries that are difficult to achieve using other techniques **[UC2]**. Commonly, sheets of nylon coated with thermoplastic polyurethane (TPU) are used. The process does not require specialist tools **[DC1]**, although it is largely manual, and design iteration is limited due to the lack of modelling support. Furthermore, producing more complex shapes often requires expert knowledge of pattern design or specialised sealing tools [48, 112]. Unlike the previous two interface types, heat-sealed TPU pouches are flexible but inelastic. This alters the possible interaction, limiting deformation inputs such as pulling or stretching **[UC2]**. The inelasticity significantly limits volume change under pressure, which may be desirable in some applications. Furthermore, it also has much lower internal stiffness, reducing the minimum resistance forces.

These three types of deformable interface expand the diversity of HydroHaptics applications. Designers can choose the most appropriate interface based on the intended application and interactions.

4 Fabrication and Implementation

This section describes the fabrication of HydroHaptics's core components: the electro-mechanical *Haptic Engine*, the soft *Deformable Interfaces*, and the sealed *Hydraulic Cell*. It also outlines the implementation of the bespoke hydro-mechanical control systems. To support reproducibility 3D STL files and parts lists (BOMs) are included in the supplementary materials.

4.1 Haptic Engine

The design of the Haptic Engine enables the BLDC motor to drive the rolling diaphragm via the lead screw carriage, offering a compact, modular solution adaptable to different motor sizes and travel distances. The Haptic Engine consists of two sub-assemblies: the *Motor Base* and *Lead Screw Carriage* (Figure 4).

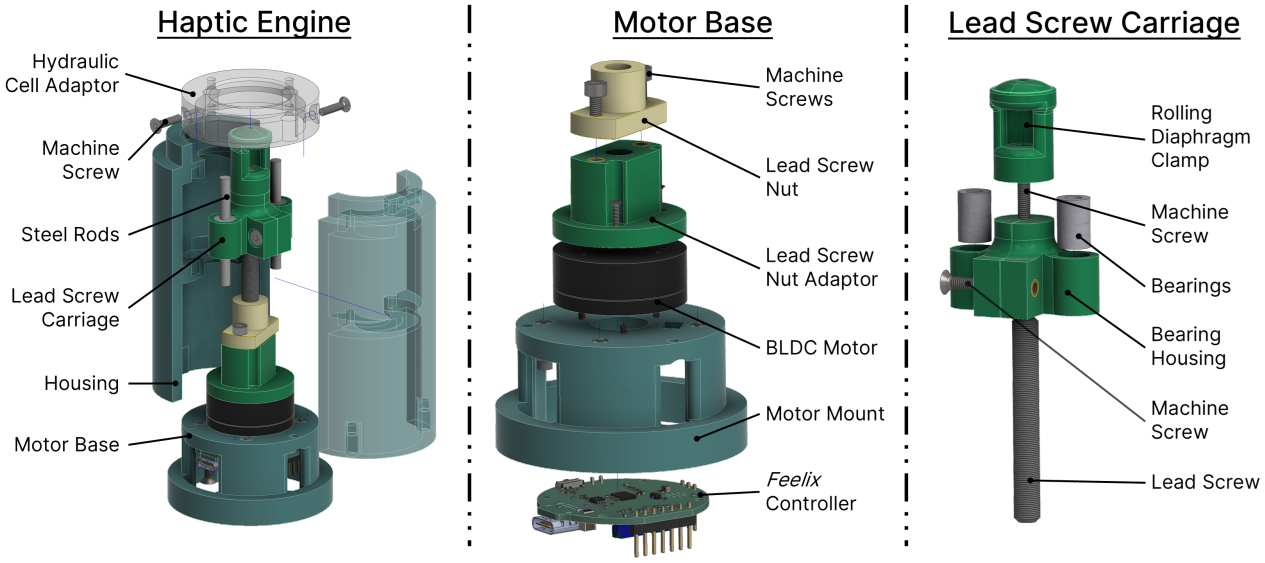

Figure 4: Exploded view of the Haptic Engine (left), as well as the two sub-assemblies: the Motor base (centre) and the Lead Screw Carriage (right). The haptic engine transmits rotary actuation into linear motion to control the rolling diaphragm.

The Motor Base (Figure 4, centre) houses the BLDC motor (ROB-20441), lead screw nut, and microcontroller. The BLDC motor's stator is secured to the motor mount—a 3D-printed PLA base positioned above the "Feelix Controller" (DRV8316 Driverboard [93]). The lead screw nut [1] is directly driven via the Lead Screw Nut Adaptor—a rotor-mounted adaptor with heat-set threaded inserts.

The Lead Screw Carriage (Figure 4, right) connects the Motor Base to the rolling diaphragm. This consists of the Bearing Housing and Rolling Diaphragm Clamp, both 3D printed PLA with embedded threaded inserts. Two press-fit 8mm linear Bearings constrain the rotation while allowing smooth sliding along steel rods. The steel Lead Screw [2] passes through the Bearing Housing and is clamped in place. Motor rotation drives the Lead Screw nut, moving the Lead Screw Carriage up and down which changes the shape of the rolling diaphragm and therefore the pressure in the Hydraulic Cell. Finally, the Housing (Figure 4 left) aligns the Steel Rods with the Motor Base and consists of two 3D printed PLA halves and a hydraulic cell adaptor with threaded inserts for secure mounting.

4.2 Deformable Interface

We used three different fabrication methods for the deformable interface, previously introduced in subsection 3.6.

4.2.1 Silicone Construction. We made the silicone deformable interfaces (Figure 5A) using EcoFlex [3], a two-part, room-temperature-curing silicone. We mixed the silicone before purging the air using a degassing chamber to prevent gaps in the final interface. We then poured this into a PLA mould, ensuring all gaps were filled before a second degassing step was performed to release any trapped air.

4.2.2 3D-printed TPU. We 3D printed a deformable interface from TPU (Figure 5B) using a similar process for 3D printing a rigid part. We created a model in CAD software before slicing and printing on a Sovol SV06 Plus[4] and a Prusa MK3S printer[5], using AzureFilm TPU 85A[6] and NinjaTek NinjaFlex TPU 85A[7], which were dried when required to improve print quality. We achieved airtight parts by printing in vase mode which ensured there were no gaps in the print where air could escape because each layer of the print was laid down continuously in a loop.

[1] igus. *Lead Screw Flange Nut – drylin SD.* Retrieved July 14, 2025, from https://www.igus.co.uk/drylin-sd/lead-screw-flange-nut
[2] igus. *Lead Screw – drylin SD.* Retrieved July 14, 2025, from https://www.igus.co.uk/drylin-sd/lead-screw
[3] Smooth-On. *Platinum Silicone Rubbers – EcoFlex Series.* Retrieved July 14, 2025, from https://www.smooth-on.com/category/platinum-silicone/
[4] Sovol. *Sovol SV06 Plus Fully Open Source 3D Printer with Linear Rail Structure.* Retrieved July 14, 2025, from https://www.sovol3d.com/products/sovol-sv06-plus-fully-open-source-3d-printer-with-linear-rail-structure
[5] Prusa Research. *Original Prusa i3 MK3S.* Retrieved July 14, 2025, from https://www.prusa3d.com/category/3d-printers/
[6] AzureFilm. *Flexible Filament 85A Blue.* Retrieved July 14, 2025, from https://azurefilm.com/product/flexible-filament-85a-blue/
[7] NinjaTek. *NinjaFlex Flexible TPU Filament.* Retrieved July 14, 2025, from https://ninjatek.com/shop/ninjaflex/

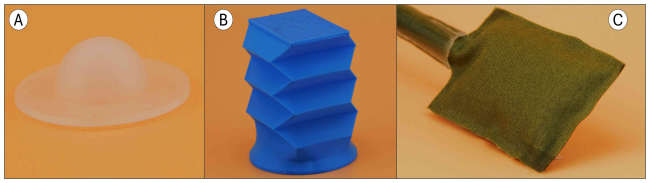

Figure 5: The three different Deformable Interface fabrication methods: (A) Cast silicone rubber to form an elastic dome; (B) 3D printed in vase mode from TPU filament to form a harmonica design and; (C) two sheets of TPU Fabric heat-sealed to form a rectangular pouch.

4.2.3 TPU Fabric Construction. Finally, we created TPU fabric interfaces (Figure 5C) by bonding together sheets of TPU-coated nylon with a heated (260-270°C) iron to form sealed pouches. A layer of heat-proof paper was placed between the fabric and the iron to prevent surface damage, and the iron was run over the seam to melt and bond the layers of TPU.

4.3 Hydraulic Cell

The hydraulic cell contains a fixed volume of liquid that transmits the force between the haptic engine and the deformable interface. The cell was designed to be robust and airtight while enabling connections between different system elements. Below we describe the implementation and fabrication of the different elements of the hydraulic cell.

Rolling Diaphragm. The Rolling Diaphragm (Figure 3) is cast from 30A Ecoflex silicone. A two-part mould is used to create the required negative and allow for the moulded part to be removed at the end. It uses the same casting process as described in subsubsection 4.2.1.

Hydraulic Manifolds. The hydraulic manifolds (Figure 2) are dual-purpose; they both provide water-tight containment for the hydraulic liquid and provide mounting points for other components, such as sensors or connectors. The manifolds are 3D-printed from PLA, and the internal surfaces of the Hydraulic Manifolds are sprayed with a clear lacquer to seal them. Threaded inserts are embedded into the surface at clamping faces to provide connecting points for bolts.

Hydraulic Tubing. Widely available polyurethane tubing can extend the hydraulic cell, connecting separate hydraulic manifolds together. tubing connects different elements of the hydraulic cell. The tube allows for the haptic engine and deformable interface to be separated (Shown in Figure 1C), moving rigid components in the engine away from interactive devices—removing the need to have rigid components inside of a soft object. Furthermore, it lets the engine and interface move relative to each other, facilitating more mobile applications.

Filling the Hydraulic Cell. The system must be completely filled with water, as air trapped within the system increases compressibility and degrades performance. We developed two methods to achieve this. The first involves fully submerging the hydraulic cell in water, allowing any trapped air to escape before sealing it underwater to prevent air from re-entering. The second, more reliable approach uses a raised, open-topped filling reservoir connected to the hydraulic cell via tubing. As water flows in from the reservoir, air can also escape upward through it. Agitating the system helps release trapped air, and the haptic engine's position can be adjusted during filling to set its default state.

4.4 Control System Implementation

4.4.1 Force Output Control. HydroHaptics employs a multi-level control architecture (Figure 6) to render force feedback. At the top level, pressure effects define the relationship between force output and user input (displacement, time). These effects can be manually set or designed using an updated version of the "Feelix" haptic authoring tool [94] (described below). The control system combines the pressure effect with the system state to compute the target hydraulic cell pressure, similar to other haptic systems.

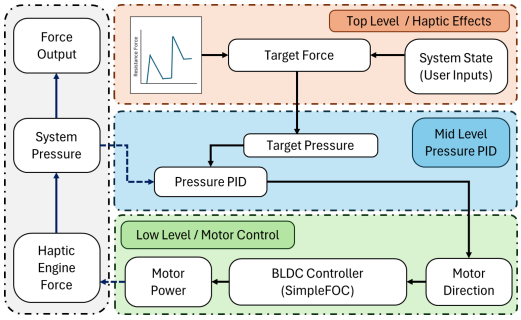

Figure 6: Control architecture of HydroHaptics. There are three levels of control, highlighting how haptic effects are rendered as changes in internal pressure.

4.4.2 Internal Pressure Control. The haptic engine can dynamically change the pressure inside the hydraulic cell by applying a force through the rolling diaphragm. This results in a force output at the deformable interface, allowing the system to render different stiffness levels. In the mid-level control, HydroHaptics utilises a Proportional-Integral-Differential (PID) controller to continually adjust the haptic engine position to maintain a target internal pressure. At the low-level, a controller based on the SimpleFOC open-source system drives the BLDC motor, forming a closed loop with the pressure PID that tracks the target force, abstracting low-level control and allowing designers to focus on force output.

4.4.3 Sensing. HydroHaptics's sensors serve two purposes, first enabling closed-loop control (as described previously) and second detecting user inputs. To achieve this, HydroHaptics employs pressure and volume sensing. Hydraulic cell pressure is measured using low-cost (<£20) Honeywell ABP [8] hydraulic sensors embedded in either the cell wall or connecting tubes, providing continuous pressure monitoring. Volume is inferred from the motor position, tracked by an AS5048A magnetic position sensor. Since the rolling diaphragm is mechanically linked to the BLDC motor, the diaphragm position can be precisely determined from the motor position. These sensing mechanisms enable closed-loop pressure control and continuous user input monitoring, feeding into the target force calculations.

4.4.4 MicroController. The system uses the open-source "Feelix Driver Board" [93], which has an onboard DRV8316 motor driver, AS5047D position sensor and STM32F401RCT microcontroller. The driver board is designed to control low voltage (up to 20V) brushless motors that operate at low speeds, deliver high torque, and have an internal resistance of approximately 10 Ohms or higher. The 40 mm diameter board is packaged within the haptic engine housing directly below the motor. This removes the need for multiple external boards and significantly simplifies the implementation.

[8] Honeywell. *Basic ABP Series Board Mount Pressure Sensors.* Retrieved July 14, 2025, from https://automation.honeywell.com/gb/en/products/sensing-solutions/sensors/pressure-sensors/basic-abp-series.

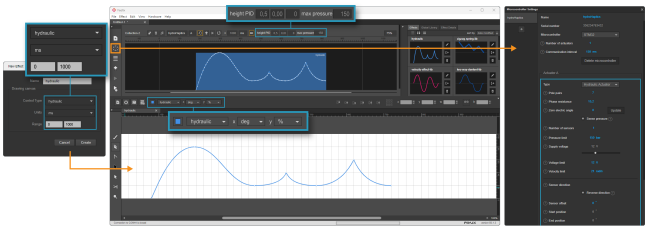

Figure 7: The updated Feelix haptic effect authoring tool. This facilitates the authoring of *pressure-based effects*, which define a relationship between user input displacement and hydraulic cell pressure, resulting in dynamic force feedback as the interface is deformed.

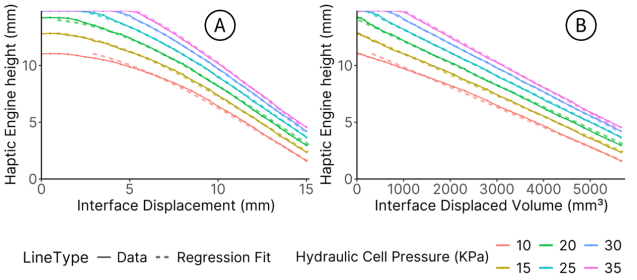

Figure 8: Interface displacement (A), and calculated interface displaced volume (B) versus haptic engine position, comparing measured values with regression model predictions across a range of hydraulic Cell pressures.

4.5 Haptic Authoring

Authoring tools can be used to design pressure effects that are operationalised by the Haptic Engine [**D3**]. While prior works have considered this on passive [47, 120] devices. Leveraging the PID pressure control and input sensing, *pressure-based effects* can be created, defining how internal pressure changes in response to user input. When uploaded to HydroHaptics, the internal pressure dynamically adjusts based on input—according to the pressure-based effects, producing a force output profile the user can feel. We look to "Feelix" [94], an open-source platform for authoring rotating rotary effects on dials. Feelix provides a GUI to author, edit and upload haptic effects to a rotary dial, as well as allowing the current input to be visualised. We adapted Feelix to support HydroHaptics, enabling users to author deformable pressure effects while visualising the current input displacement (Figure 7).

5 Technical Evaluation

We evaluated how accurately and precisely HydroHaptics can render force feedback on deformable interfaces through a series of technical evaluations. All tests used a configuration of HydroHaptics (shown in Figure 2), comprising the ROB-20441 motor, a 2.54 *mm* pitch lead screw, and a 13 *mm* radius silicone dome interface. Evaluations were performed using a UR3 robotic arm equipped with a Nordbo NRS-6 six-axis force sensor. An oval-shaped probe, approximating the size of a human index finger [100], was mounted on the arm for all measurements. During the testing, the pressure inside the hydraulic cell was set and adjusted using the PID control (described in subsection 4.4). Data from both HydroHaptics and the robot arm setup was collected at 5 *ms* intervals.

5.1 Test 1: Volumetric Input Sensing

We begin by assessing how precisely HydroHaptics can estimate the deformation of the interface based on the movement of the Haptic Engine during user input. The robot arm (simulating a user) compressed the interface in 0.5 *mm* increments from 0 to 15 *mm*, and we measured the probe displacement, internal pressure and haptic engine position over a 200 *ms* window at each increment. Each compression depth was tested at six different hydraulic cell pressures—5 *kPa* steps from 10 to 35 *kPa*, and each combination of pressure and depth was repeated five times. The average standard deviation across all points was 0.6% of pressure, with a maximum of 2.2%, demonstrating internal pressure stability during testing. As the robot arm compressed the dome-shaped interface, the volume of displaced fluid increased non-linearly with displacement. This can be calculated using the equation for the volume of a spherical cap [104], reflecting the increase in cross-sectional area with depth. Figure 8 shows the relationship between the position of the haptic engine and robot arm displacement (A), and calculated volumetric displacement (B). The plateaus observed at the higher pressures occur as the haptic engine's maximum position does not provide the required pressure. Only when sufficient input is provided does the pressure in the hydraulic cell start to match the target pressure, at which point the motor begins moving to regulate the pressure. Interestingly, the results show a linear relationship between volumetric displacement and the haptic engine's position. Therefore, we created a linear regression model—excluding the initial 2 *mm* displacement region due to high variance—to predict volumetric displacement of the deformable interface based on the hydraulic cell's pressure and position of the haptic engine. The model demonstrated excellent accuracy, with a standard deviation of 0.18 *mm* across all tested haptic engine positions and hydraulic cell pressures. These results confirm that HydroHaptics can reliably estimate how much a user deforms the interface based on the hydraulic cell pressure and haptic engine position.

5.2 Test 2: Pressure to Force Testing

Next, we assess how accurately and precisely the haptic engine can control and regulate the pressure of the hydraulic cell. This is important for providing different levels of stiffness. The robot arm compressed the interface to a depth of 10 *mm* while the system commanded pressures from 0 to 40 *kPa*, increasing in 2.5 *kPa* increments. For each pressure level, the internal pressure of the hydraulic cell and output resistance force—sensed by the robot arm probe—were recorded over a 200 *ms* window, with 10 trials per pressure level. Figure 9 shows the target pressures against measured pressure (A) and measured output force (B). These results show an average error of -0.27 *kPa* (≈.5% full scale) with an average standard deviation of 0.23 *kPa* over the range. A linear regression was used to predict the relationship between target pressure and measured force, with a root mean square (RMS) error of 0.17 *N* across all

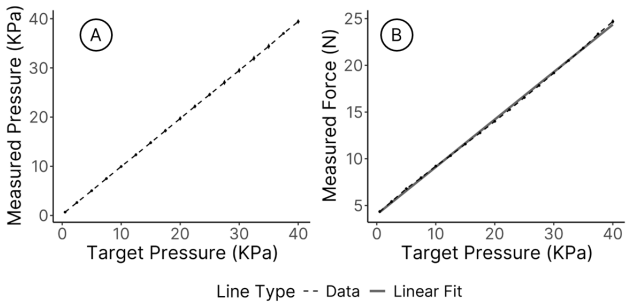

Figure 9: Target pressure vs. pressure measured inside the hydraulic cell (Measured Pressure) (A) and the force measured from the robot arm force sensor as it compressed the cell (Measured Force) (B). A linear regression was fit between target pressure and measured force.

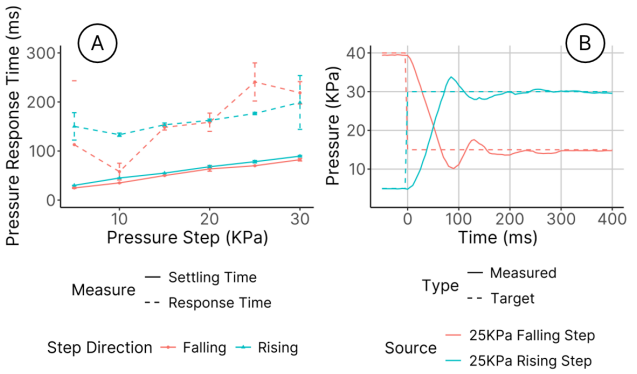

Figure 10: Step response performance for pressure (A) showing both response and settling times. An example response graph is also shown for pressure falling from 40 kPa to 35kPa and rising from 10 kPa to 35 kPa (B).

pressure levels. These results confirm HydroHaptics's ability to accurately and precisely control internal pressure which linearly translates to the interface resistance force a user feels across a wide pressure range, demonstrating its capability to provide accurate, high-fidelity force feedback.

5.3 Test 3: Step Response Time

The third test measures the step response performance which indicates how quickly the haptic engine can change the pressure in the hydraulic cell. The dome was compressed by 10 *mm*, before the target pressure was changed, and the response time (the time to first reach within the target pressure limit) and settling time (time to settle within the limit) were calculated as measured by the hydraulic cell pressure with a 1 *kPa* tolerance. We measured both rising (starting from 5 *kPa*) and falling (starting from 40 *kPa*) pressure changes, with the target pressure varying over six steps from 10 *kPa* to 35 *kPa*. Ten trials were conducted per pressure step.

The results are shown in Figure 10, including example profiles of rising and falling edges. The response time increased with pressure difference, ranging from 20 *ms* to 100 *ms*, with settling times around 100 *ms* slower at higher pressure levels. This pressure response performance can be combined with the results from Test 2—showing the linear relationship between internal pressure and output force—to understand the dynamic force-feedback capabilities of HydroHaptics. Previous pneumatic systems have demonstrated step changes of 800 ms for transitions between 1.5 and 5.5 *N* [14], and 300 ms to transition between 0.2 *N* and 1.4 *N* [121]. In contrast, HydroHaptics achieved transitions from 5 *kPa* (7 *N*) to 30 *kPa* (19 *N*) in under 100 *ms*. This highlights how HydroHaptics can achieve fast step response times meaning force feedback and stiffness can be changed dynamically on-the-fly.

5.4 Test 4: Frequency Response

Finally, we analysed the frequency response of HydroHaptics to understand the maximum frequency of oscillatory force feedback that can be provided. We used the approach described by Zhu et al. [121]. We tested 20 frequencies spaced logarithmically from 1 *Hz* to 50 *Hz* across five different pressure amplitudes (from 2.5 to 17.5 *kPa*) to explore the interaction between frequency and force. The robot arm compressed the dome to 10 *mm*, and the hydraulic cell pressure was measured over a 2 s window for each unique pressure and frequency combination. A fast Fourier transform (FFT) was applied to each trial to determine the magnitude of the force response at the target frequency. The results are presented in Figure 11, along with example frequency response profiles. Combining again with the results from test 2, we can understand the force-feedback implications. The results demonstrate that HydroHaptics can reliably render a 2.5 kPa (1 *N*) amplitude wave up to 10 *Hz* and a 12.5 kPa (6 *N*) amplitude wave up to 5 *Hz* with only minor distortion. They also illustrate the decrease in maximum achievable amplitude at higher frequencies, showing approx 3 kPa (1.5 *N*) limit at 15 *Hz* and 1.6 kPa (0.6 *N*) limit at 21 *Hz*. Similar tests were conducted on "JetUnit" [119] and "PneuSleeve" [121]. "PneuSleeve" demonstrated approximately 0.2 *N* at 15 *Hz* and 0.1 *N* at 21 *Hz*. While "JetUnit" only reported performance up to 10 *Hz*, achieving approximately 0.5 *N* of force. This test demonstrates that HydroHaptics is capable

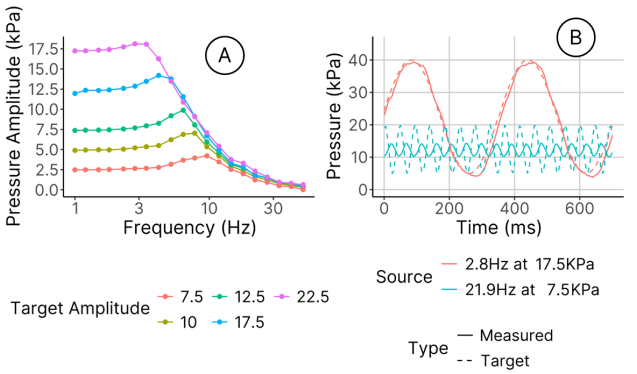

Figure 11: Frequency response performance for HydroHaptics on a logarithmic scale (A). Example plots show the frequency response at 2.8 Hz, 17.5 kPa and 21.9 Hz, 7.5 kPa (B).

of rendering dynamic oscillatory force feedback with high accuracy, consistently achieving precise frequency matching up to 5 Hz across a wide range of forces. This enables the delivery of distinct haptic outputs through various pulsing signals.

5.5 Summary

The technical evaluation demonstrates the clear advantages of hydrostatic transmission for force feedback, as well as the performance of HydroHaptics. Test 1 confirmed how HydroHaptics can accurately and precisely sense input based on the haptic engine's position, while Test 2 demonstrates how the haptic engine can transmit force in a predictable way to the deformable interface without loss and distortion, over a wide range of pressures. Test 3 illustrates how HydroHaptics can provide responsive and dynamic changes in internal pressure, achieving rapid adjustments in output within short time intervals. Test 4 demonstrates how HydroHaptics can accurately vary its internal pressure at frequencies exceeding 10 Hz. Collectively, these findings show how HydroHaptics advances the force feedback performance possible on macro-fluidic deformable interfaces, opening up unique opportunities for interaction.

6 User Study

The technical evaluation characterises the high precision of HydroHaptics's system pressure and input displacement sensing and demonstrated high-fidelity and responsive force feedback. To understand the user experience of HydroHaptics, we conducted a two-part user study examining both how users perceive different types of force feedback and how accurately the system can detect different input gestures that can enable unique interaction possibilities. Both parts were completed by the same group of participants using a single study setup, with only minor modifications between them (detailed below). The studies were run sequentially, beginning with the force feedback component. Each part addressed a distinct research question: the force feedback study explored the perceivability and distinctiveness of pressure effects rendered by HydroHaptics, while the input study evaluated the system's ability to recognise user-performed gestures.

The study took place in an office at the research institution, and participants were recruited using internal institution advertising. The participants sat in an office chair with the HydroHaptics prototype embedded into a frame in front and slightly to the side, positioned so their dominant hand would rest comfortably on the dome (Figure 12). The chair could be moved to either side of the frame depending on the participant's handedness. The top of the prototype was flush with the surface of the frame, with only the silicone dome extending above the surface (Figure 12B).

6.1 Participants

We recruited 18 participants (11 identified as female, 7 identified as male), aged between 19 to 54 (Mean = 30.6, σ = 10.5). All had full mobility of their index finger on their dominant hands, with 17 right-handed and one left-handed. They were compensated with £10 each for taking part in the study.

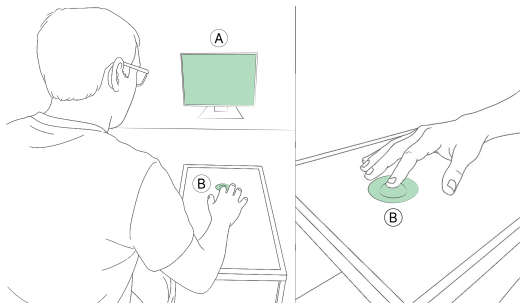

Figure 12: The user study setup. The HydroHaptics prototype is sunken within a frame, with only the dome (B) extended above the surface. The participant is sat to the side of the frame, facing the display (A).

6.2 Force Feedback Study

As demonstrated within the technical evaluation, HydroHaptics can accurately control the resistance force felt when compressing the interface by altering the pressure inside the hydraulic cell. Building upon this, we evaluated whether pressure effects produced by HydroHaptics—which would be felt as varying force feedback—were distinguishable by users. This study section tasked participants with identifying different effects, following the approach of Chen et al. [10]. Drawing on related work and our understanding of HydroHaptics's capabilities, the six pressure effects (shown in Figure 13) were designed to demonstrate a range of feedback behaviours. Three of these were displacement-dependent, varying in response to user input, while the remaining three were system-controlled, varying over time and independent of input. They are described in more detail below.

6.2.1 Pressure Effects. **Clicks** introduce small drops in resistance at discrete displacement increments, a common mechanism for indicating increments [94, 120]. **Boundary** increases the resistance beyond a set depth, simulating physical limits similar to those used in constrained dials [95]. **Button** simulates the familiar tactile response of a physical button [1, 45], with a rise and sudden drop in resistance at the actuation point. **Bumps** generate brief tap-like pulses using short square waves, similar to notification feedback [8, 121]. **Oscillating** provides rhythmic force feedback that can guide pacing or focus attention, as in breathing aids [17]. Finally, **Stiffening** gradually increases resistance over time, signalling prolonged interaction and subtly discouraging continued input in focus-critical contexts.

6.2.2 Study Methodology. During the study, the participant's hand and the prototype were obscured from view using a box to eliminate visual cues. Participants also wore noise-cancelling headphones to minimise auditory cues, ensuring the user study results reflect haptic perception alone, following prior work [119]. At the beginning of the study, participants were familiarised with the six Pressure Effects; each effect was demonstrated at least twice, with additional demonstrations provided upon request. Once ready, participants felt the pressure effects rendered by the device and verbally identified each effect, which the researcher entered into the study software. Participants were not informed of the correctness of their answers

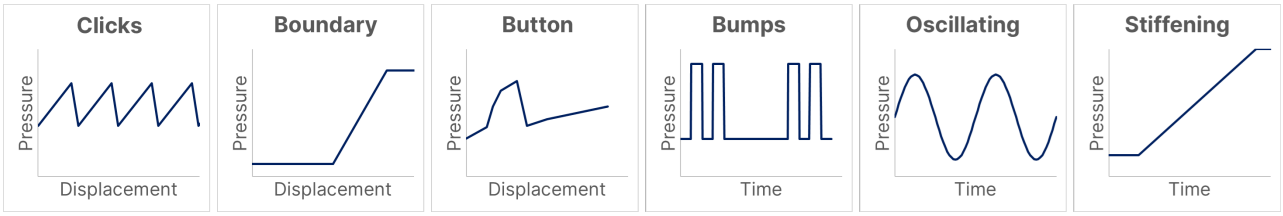

Figure 13: The six pressure effects rendered to users in the Force Feedback Study. The first three effects are displacement-dependent, changing as the user pushes into the device. The second three are time-dependent and change independently of user input.

during the trials. Additionally, participants received a physical sheet showing the six graphs from Figure 13, each accompanied by its name, as the task was designed to evaluate the distinctiveness of each effect rather than memory recall. Effects were presented in blocks, each containing all six effects in a random order. Each participant completed 10 blocks, resulting in a total of 60 trials per participant. During the study, we measured if the participant identified the correct pressure effects (Success) and, the time taken for the participant to make their selection (Response Time).

6.2.3 Results. We analysed *success* using a binomial logistic generalised linear mixed model, as success is a dichotomous outcome and, therefore, unsuitable for analysis with repeated-measures ANOVA. We created a model of success with *pressure effect* as a fixed effect and participant as a random effect, which had an explanatory power of $Cond.R^2 = .406$ for both fixed and random effects and $Marginal.R^2 = .079$ for the fixed effects alone (Nakagawa and Schielzeth [55]). The overall success across all trials was $\mu = 82.6\%$ [80.3%, 84.9%], ranging from the *Oscillating* effect ($\mu = 92.8\%$ [89.0%, 96.6%]) to the *Boundary* effect ($\mu = 69.3\%$ [62.4%, 76.1%]). There was a significant effect of PRESSURE EFFECT on success ($\chi^2(5) = 51.75$, $p < .001$, $R^2_{sp} = .048$ [9]). Individual post hoc comparisons are shown in Table 1. A confusion matrix summarising participants' responses is shown in Figure 14, illustrating the distribution of user responses versus the true effect. This highlights the distinctiveness of certain effects such as *Oscillating*, *Stiffening*, and *Buttons*, while also revealing notable misclassifications—e.g., the *Boundary* effect was misidentified as *Stiffening* in over a quarter of the trials.

[9] R^2_{sp} calculated following Stoffel et al. [86]

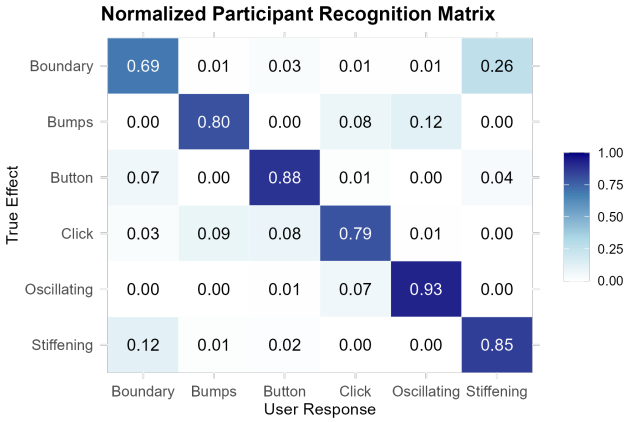

Figure 14: Normalised participant response distribution for the six haptic effects.

For *response time*, we began by checking the data against the assumptions of a one-way RM ANOVA. A Shapiro–Wilk test indicated that the data were not normally distributed and could not be corrected with transformations. Therefore, we used a Friedman test to analyse the response time data, with Holm–Bonferroni-corrected Wilcoxon signed-rank tests for post hoc analysis. Across all trials, the median response time was 7.27 s[6.93 s, 7.61 s]. There was a significant ($\chi^2(5) = 50.8$, $p < .001$, $W = 0.58$) effect of PRESSURE EFFECT on response time. Post hoc tests revealed significant differences between several condition pairs. Bumps ($m = 4.73$ s [4.38 s, 5.07 s]) and Oscillating ($m = 4.94$ s [4.48 s, 5.40 s]) were identified fastest, while Boundary ($m = 9.66$ s [8.73 s, 10.60 s]) and Clicks ($m = 9.32$ s [8.23 s, 10.40 s]) took the longest.

6.2.4 Summary. These results demonstrate the ability of HydroHaptics to render distinct pressure effects, including oscillating, buttons and stiffening, which users can very consistently identify. This aligns with the results from the technical evaluation, which demonstrated that the system could create changes in output force by altering the internal pressure. It also highlighted how certain gestures can be more difficult for users to identify and can commonly be mistaken for others. This both validates the haptic capabilities of HydroHaptics and provides insight into the design of distinct haptics on the device.

6.3 Recognition of Deformable Gestures

The technical evaluation confirmed the precisions of HydroHaptics's force and displacement sensing. Noteworthy, deformable inputs provide users with a rich interaction space, enabling a diverse range of gestures that are not limited to a single input type. Therefore, we wanted to understand the feasibility of HydroHaptics to differentiate between these different inputs accurately. As an initial investigation into the ability of HydroHaptics to detect gesture inputs, we selected four gestures and trained a machine learning classification model to identify them. The four gestures, Press, Pinch, Shear and Twist, are shown in Figure 15 and were selected as they are both common and well-suited to a simple deformable dome.

6.3.1 Data Collection Methodology. To begin, participants completed a familiarisation phase, during which the researcher introduced and demonstrated the four input gestures. This was followed

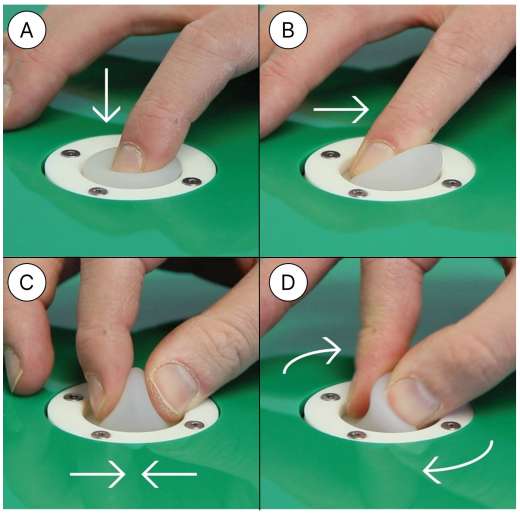

Figure 15: The four gestures performed in the Deformable Gestures Recognition study. Press (A), Shear (B), Pinch (C), Twist (D).

by a short practice period before proceeding to the recognition task. Participants were promoted to perform the tasks as if they were interacting with an everyday device. The participant was shown a prompt on a display (Figure 12A) stating which gesture to perform. The four gestures, along with 'no gesture'—used to collect baseline data—were shown together in a random order within a single block. During the 'no gesture' condition, the participant completely removed their hand from the interface and did not touch it for the duration of the gesture. The participant was shown 15 blocks overall, for a total of $4 \times 15 = 60$ gestures per participant, and 60×18 participants $= 1080$ gestures collected in total. The Researcher controlled the study, beginning and ending the recording for each trial. During each gesture, the system measures the pressure, motor height and motor voltage every 5 *ms*. The collected data was visually inspected after the test was complete to ensure all files had complete data within them, with participants being asked to repeat specific gestures if they were missing or incomplete.

6.3.2 Gesture Classifier. We trained a Random Forest classifier (n = 300) using 'scikit-learn' [64] to recognise gesture type from the time-series pressure and haptic engine height data. A touch flag signal—which identifies touches based on the movement of the motor—was used to segment the gesture, with each gesture window beginning 100 *ms* before the first contact and ending 200 *ms* after the user released. The "Blank" gestures were omitted from the classification. To capture temporal dynamics, each gesture was divided into $N = 3$ overlapping subwindows (50% overlap) to split between the initial dip, hold and release. We perform feature extraction on each window, calculating the minimum, maximum, mean, and standard deviation for both pressure and height.

6.3.3 Results. To evaluate gesture classification performance, we employed two distinct evaluation protocols with contrasting train-test split strategies. For the user-dependent condition, we implemented a Leave-One-Trial-Out (LOTO) cross-validation approach,

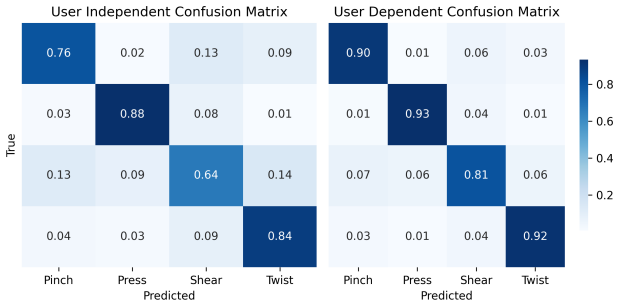

Figure 16: User-independent and user-dependent confusion matrices for the Deformable Gestures Recognition study.

where the classifier was trained on all trials from a participant except one, which was used for testing. This process was repeated for all trials of each participant, effectively evaluating how well the system recognizes consistent gestures from the same user. For the user-independent condition, we utilised a Leave-One-Participant-Out (LOPO) cross-validation approach, where the system was trained on data from all participants except one, whose data served exclusively as the test set. This process was repeated for each participant, rigorously assessing the system's ability to generalise across different users. The results revealed strong performance in the user-dependent classification (89.1%, SD = 8.11), with Pinch (93%) and Twist (92%) gestures achieving the highest recognition rates due to their distinctive motion patterns. However, Shear gestures performed less effectively (81%), likely due to inconsistencies in execution or overlap with other gestures. In the user-independent condition, accuracy decreased notably (77.8%, SD = 10.57), highlighting the challenge of accommodating diverse gesture execution styles across users. While Twist remained relatively robust (84%), Press exhibited significant challenges (64%), frequently being misclassified as Shear. An example of live gesture recognition is shown in the video figure.

6.3.4 Summary. Our gesture classification system, employing a simple classifier, achieves a promising performance while prioritising interpretability and ease of deployment. However, performance variability, particularly for Shear and Pinch gestures in user-independent protocol, reveals areas for further improvement. While this approach is limited to only four gestures classified post-hoc, it demonstrates how user input can be recognised to facilitate deformable gestures alongside high-fidelity force feedback without adding additional sensing. Future work could explore deep learning or hybrid models to better capture the nuances within these gesture classes. Furthermore, adaptive mechanisms like personalised calibration may help address inter-user variability. Larger, more diverse datasets could also enhance the system's generalisability.

7 Applications

The HydroHaptics platform expands the interaction space for deformable devices. We present four unique applications which utilise the technical capabilities and design features described in this paper.

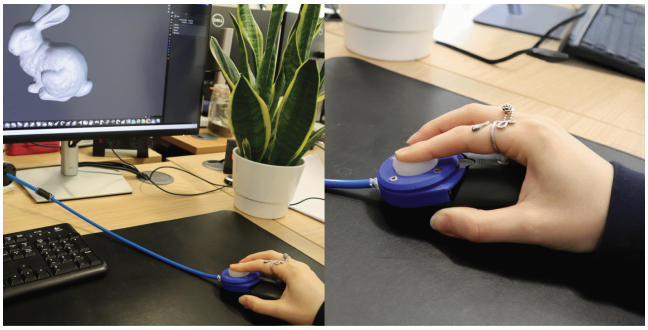

Figure 17: 3D Sculpting Deformable Mouse, which enables bi-directional force-augmented sculpting of digital objects. It supports force-based sculpting and deformable gestures while providing continuous, dynamic force feedback.

7.1 3D Sculpting Deformable Mouse

We built a deformable mouse (Figure 17) for 3D sculpting, combining prior concepts of deformation sculpting [28] and the "Inflatable Mouse" [41]. A silicone dome is mounted on a hydraulic cell at the front of a standard computer mouse, preserving the mouse's spatial interaction capabilities. The device supports bi-directional force-augmented interactions with enhanced deformable force-feedback while retaining the traditional discrete button input and "button" feedback effect (Figure 13). Beyond confirming inputs, the device can render continuous force feedback to simulate the stiffness of the virtual material, allowing users to haptically explore the digital object with the same tool used to modify it. Subtle haptic cues can also be conveyed—such as "taps" when nearing the base of a model or "stiffening" when sculpting restricted regions—enhancing situational awareness during the creative process. This enhanced force feedback is complemented by HydroHaptics' ability to provide users with greater flexibility in how they provide input through the deformable interface. This enables continuous deformable force input during sculpting, allowing users to modulate the thickness of a stroke based on the force of the input. In addition, deformable gestures (Figure 15), such as shearing to switch brushes or pinching to move objects, further expand the expressivity.

7.2 "Wayfinding" Force-augmented Backpack

We implemented a force-augmented backpack (Figure 18), which builds on prior work such as "ShoulderTap" [87], which delivered pneumatic on-body directional cues, and other similar wearable force-feedback systems [38, 65]. Each shoulder strap contains a heat-sealed TPU pouch embedded beneath the fabric, independently controlled by a dedicated HydroHaptics haptic engine. The straps can render a variety of force-feedback effects either independently or simultaneously. For example, oscillations on one shoulder can guide navigation, with the frequency increasing as the user approaches a turn, while taps on both shoulders prompt the user to stop or turn around. The device can also deliver variable stiffness "pushes" onto the wearer's shoulder, to provide less urgent notifications [38], with the force applied increasing with the number of notifications. In addition to output, the straps retain the HydroHaptics input capabilities. Continuous force input can be used to dismiss a notification by pressing one strap which is confirmed by a tactile button effect. Holding gestures can be used to provide multi-level input, with the bag guiding the user through the different levels by discrete click feedback, allowing for interactions such as controlling the volume of their earphones.

Figure 18: The "Wayfinding" Force-augmented Backpack provides tactile on-body feedback from force applied through a backpack strap, facilitating spatial and temporal notifications while integrating into an existing backpack. The white dashed line indicates the outline of the embedded TPU pouch.

7.3 Interactive Force Feedback Cushion

We developed an interactive cushion (Figure 19) that supports deformation-based input and force feedback, aimed at smart-home control [9]. A heat-sealed TPU pouch is embedded within the cushion and connected to the haptic engine via flexible tubing, ensuring no rigid components impact its softness. Dynamic force feedback enhances discrete and continuous force input on the cushion. Discrete inputs—such as turning off the lights—are confirmed with tactile "clicks", while rate-controlled interactions—such as scrolling through a page [3] or item selection [12, 108]—are accompanied by varying-frequency oscillations to reflect input intensity or speed. Furthermore, the cushion's physical stiffness can be adjusted using

Figure 19: Interactive Force-Feedback Cushion, that enables tactile input and feedback using a soft deformable pouch, without compromising the cushion's original softness. The white dashed line indicates the outline of the embedded TPU pouch

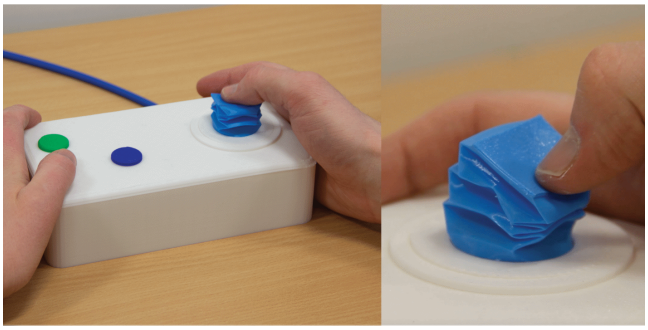

Figure 20: Deformable Joystick mock-up, which supports three-dimensional deformation input while providing immersive force feedback.

force-augmented inputs, allowing control over the level of support it provides when sat on. Beyond control, the cushion can also serve as an immersive feedback device. Oscillations, pulses, and taps delivered through the surface can be synchronised with media—such as music, films, or TV programmes—to create a more engaging experience, akin to 4D cinema.

7.4 Deformable Joystick GamePad

We implemented a low-fidelity mock-up prototype of a deformable joystick (Figure 20) using a 3D-printed TPU bellows-style interface, capable of deformation in three dimensions without requiring complex mechanical assemblies. Inspired by soft "origami" interfaces [113], our design extends the concept by integrating force feedback. The joystick can support rich, continuous deformation input enhanced by dynamic haptic feedback. Deformable force feedback can augment inputs by providing tactile confirmation and resistance—for example, pushing against a virtual object may require effort, while "bursting" involves overcoming a sudden force threshold. Furthermore, HydroHaptics could deliver immersive cues. Pulsing feedback (oscillations) can simulate tension, such as a rising heartbeat, while taking damage in-game is emphasised by sharp pulses (taps) of force on the user's finger. Such nuanced input-output coupling would be difficult to achieve with conventional mechanical joysticks, requiring substantial mechanical complexity to support similar levels of flexibility and feedback.

8 Discussion

8.1 Summary

The technical evaluation demonstrates how hydrostatic transmission can be used to simultaneously sense and measure user input (Test 1) while accurately controlling the amount of force feedback (Test 2) with a response rate of less than 100 ms (Test 3). The magnitude and range of dynamic force feedback that HydroHaptics can provide on a deformable interface exceed the capabilities of prior deformable devices, which have instead focused on providing spatial variations on a fixed form factor [59, 118]. Notably, HydroHaptics surpasses "JetUnit" [119], another hydraulic system, by exhibiting a reduced force output loss at higher frequencies (Test 4).

The user study demonstrates how users can correctly identify force feedback effects and that the HydroHaptics concept can be used to recognise a variety of deformable gestures. However, some haptic effects (e.g., Boundary and Stiffening) are more nuanced and were frequently confused by users, and some gestures—such as Shear—were more difficult to classify reliably. Prior work has explored deformation and force sensing on soft surfaces [15], however HydroHaptics demonstrates how it is possible to translate these capabilities into gesture recognition without augmenting the device with additional sensors. As deformable interfaces allow a wide range of manipulations, this creates unique opportunities to recognise diverse user input and respond in different ways.

The gesture space enabled by a deformable interface emerges from its physical properties, such as shape, size, and stiffness [44, 90, 96]. In this work, we focused on a small set of input gestures and feedback profiles, selected based on prior research and our experience. Further investigation is needed to understand how device form, input gesture, and feedback profile interact, and how these aspects can be combined to enhance the user experience.

For instance, the type of interaction and the associated feedback could be modulated dynamically during the gesture—a pinch might produce a single click, while a press could yield multiple levels of feedback. Different gestures which map to different interactions could trigger distinct tactile confirmations, giving users immediate feedback that their intended gesture was correctly recognised.

Together, these studies validate both the suitability of hydrostatic transmission for bidirectional force transfer and our implementation of HydroHaptics for rendering detailed force feedback on deformable devices. They show that force from the device can be both accurately rendered and perceptible and that user inputs can be sensed with minimal loss—enabling effective gesture recognition.

8.2 Technical Limitations

Despite the advantages described in this paper, we identified technical limitations with our specific implementation of HydroHaptics. First, air can be trapped within the hydraulic cell or leak into the system over time. The air introduces compressibility and reduces performance, requiring careful and secure system sealing. Along with this, high output pressures require significant power—especially with low mechanical advantage—which can lead to thermal issues within the haptic engine and risk damaging PLA components. While heat sensing and heat-resistant PLA offers partial mitigation, thermal management remains challenging with such high power requirements. Finally, our approach relies on a rigid haptic engine to generate force feedback. This can be separated from the deformable hydraulic cell that the user interacts with via flexible tubing, but the haptic engine must remain connected to the interface. This arrangement is not always feasible for fully deformable interfaces, for example our pillow application requires the pillow to be tethered to the couch (which houses the haptic engine). HydroHaptics represents a meaningful step toward the long-term goal of achieving fully deformable haptic force feedback systems, and future work should aim to reduce the number and size of rigid components.

In contrast to micro-hydraulic systems such as "HapTag" [10], "Flat Panel Haptics" [73] and "PopTouch" [18], HydroHaptics is a

macro-hydraulics system which operates with liquid volumes several orders of magnitude larger. While we've demonstrated key advantages of such systems, macro-hydraulics in interactive devices introduces notable limitations based on the upper bounds of performance determined by the laws of fluid dynamics. The maximum fluid flow-rate is physically constrained by viscosity and pipe geometry [105], limiting responsiveness when deforming very large volumes. Also, if the haptic engine and deformable interface are at different heights, there will be a pressure differential, leading to force output discrepancies. Macro-hydraulic systems must also contain all working fluid within the system, imposing physical constraints on the device's form factor. This is in contrast to pneumatic systems which can render large volume changes by drawing from, and exhausting to, the environment [67, 70].

Finally, there is significant potential for variation in both the interface—such as form, size, material, or stiffness—and the interaction, including input gestures and haptic effects. This work has considered only a small subset of possible interaction configurations, and more research is required to fully explore this space. In particular, the physical properties of the interface may affect—or even degrade—the quality of force feedback.

8.3 Future Work

The implementation of HydroHaptics presented in this paper opens several promising avenues for future enhancement. First, combining two or more deformable cells with different force-feedback properties could enable more complex material simulation [51, 114], along with richer spatial feedback. This could be achieved by integrating multiple haptic engines or by employing mechanical or layered valves [26] to switch a single haptic engine between multiple interfaces. Next, the current interface between the BLDC motor and the hydraulic cell could be significantly simplified through the use of a rolling-rotary diaphragm [32], allowing the motor to drive pressure and volume changes directly via rotary motion. This approach may reduce the system's footprint, simplify mechanical design, and lower the component count, potentially employing direct or geared motor coupling. Finally, techniques for fabricating hydraulic devices with transmission fluid sealed inside have been demonstrated [49, 110], which offer the potential to simplify the design. Such improvements could also facilitate the development of multi-haptic-engine devices.

Future investigations could look to better support the needs of researchers and designers. The design of HydroHaptics is highly customisable, with parameters such as diaphragm size, motor performance, lead screw pitch, haptic engine travel, and tubing configuration all adaptable to suit specific use cases. However, this flexibility currently requires significant skill and manual effort. A future parameterised design tool could streamline this process by allowing users to specify design constraints—such as working volume, maximum force, response time, interface type, and system footprint—and automatically generate tailored 3D models and component lists [2, 50, 84].

A particularly exciting potential direction is the development of passive deformable haptics. Recent work on passive mechanical systems [47, 120] highlights the potential for tactile feedback without active actuation. A passive mechanism could be leveraged to replace HydroHaptics's haptic engine. This would lead to deformable interfaces that could offer tactile sensations such as detents or resistance in low-power or mobile contexts. Combined with low-power wireless sensing, this could enable fully portable haptic-enabled deformable devices. Further, the adapted Feelix authoring tool introduced in this work could be extended to output passive haptic profiles—fabricated using methods such as laser cutting, similar to the "ShapeHaptics" [120] approach.

While programming HydroHaptics currently requires a PC, future versions could enable end-users to configure the device via the deformable interface. Users could create custom haptic profiles by applying force to the interface or train new gesture classifiers using specific deformation commands.

Finally, while the current version of HydroHaptics provides haptic feedback along a single degree of freedom (DoF), extending this to multi-DoF haptics is a compelling long-term goal. Enabling different actuations across multiple directions would unlock richer and more expressive interactions. This might be achieved through structured metamaterials, combined actuation modalities, or software-driven techniques. For example, predictive sensing could detect gestures such as twisting before they are fully completed, allowing the system to adjust feedback in real-time and create the illusion of multiple output dimensions.

8.4 Towards the Future of Deformable Devices

Prior work has shown how deformable devices, with their many degrees of freedom, allow users to interact in expressive and personalised ways [44, 90, 96]. However, deformable devices have seen limited adoption outside of a research context despite their rich input expressivity [43, 98, 101] and the wide variety of form factors [17, 60, 68, 85]. We postulate that the lack of adoption is in part due to their reduced haptic feedback capabilities—this is particularly evident when contrasted with the growth in force feedback in other domains, such as haptic simulation [5, 72] and pseudo-haptic techniques [37, 83, 103].

Deformable haptics enabled by HydroHaptics, defined by their high fidelity and responsiveness, directly addresses this shortcoming. Deformable force feedback can augment and enhance existing systems and enable new interaction possibilities that were previously out of reach, helping to accelerate the wider adoption of deformable devices. Deformable devices will not completely replace rigid devices, however we believe they serve a distinct but vital role, much like soft robots do in the field of robotics [106].

Deformable devices are also particularly suited to replicating real-world objects, such as those used in training applications. For example, anatomical models or manikins are already made from soft, malleable materials [89, 92] to enhance realism. However, these devices are currently restricted to passive force feedback. Deformable haptics could transform these tools by enabling real-time changes in stiffness, even pushing users back, making training scenarios more immersive and effective.

Finally, many of the objects we interact with daily are soft—and their softness is essential to their functionality. Items like pillows, chairs, children's toys, clothing, mats, and bags rely on this quality. Augmenting them with deformable haptics could unlock exciting

new interaction opportunities. Such enhancements could extend at-hand computing, allowing us to interact with smart home systems—like thermostats, media controls, or lighting—through the soft objects already around us. They could also enable more expressive and immersive experiences, such as toys that move or push back in response to touch. Further, deformable haptics could make everyday objects more adaptable. For example, chairs that stiffen to support posture or items that soften for easy storage, enabling multifunctional and responsive designs.

By enabling deformable devices to provide force feedback on par with rigid systems, HydroHaptics removes a major limitation to their wider uptake. We believe that HydroHaptics and other future deformable force feedback technologies will fundamentally reshape the role of these devices in everyday life.

9 Conclusion

In this paper, we introduced HydroHaptics, a novel open-source system which can accurately render fine-grained haptics on deformable interfaces and devices while remaining practical and reproducible for researchers and designers. HydroHaptics leverages hydraulic transmission to couple the output of a BLDC motor to a deformable interface, bringing the haptic performance of mechanically articulated systems to soft, compliant devices.

Our technical and user evaluations demonstrate how HydroHaptics can maintain all of the benefits of deformability—softness, flexibility, and input richness—while providing precise, dynamic, and high-fidelity force feedback across a range of deformable interfaces on a scale that was not previously possible. This opens up a new and interesting design space, expanding the boundaries of what is possible with interactive deformable devices.

Both the hardware and software of HydroHaptics are open-source and designed for ease of replication; most components are 3D-printed using consumer-grade FDM printers with PLA or are off-the-shelf parts that are widely available and easily substitutable. This low-cost, accessible, and open-source approach lowers the barrier to entry for deformable haptics, and opens up new opportunities for exploration with deformable interfaces.

Acknowledgments

This project has received funding from the European Research Council (ERC) under the European Union's Horizon 2020 research and innovation programme (FORCE-UI, Grant agreement No.853063).

References

[1] Jason Alexander, John Hardy, and Stephen Wattam. 2014. Characterising the Physicality of Everyday Buttons. In *Proceedings of the Ninth ACM International Conference on Interactive Tabletops and Surfaces (ITS '14)*. ACM, New York, NY, USA, 205–208. doi:10.1145/2669485.2669519

[2] R. Anderl and R. Mendgen. 1995. Parametric design and its impact on solid modeling applications. In *Proceedings of the Third ACM Symposium on Solid Modeling and Applications* (Salt Lake City, Utah, USA) *(SMA '95)*. Association for Computing Machinery, New York, NY, USA, 1–12. doi:10.1145/218013.218018

[3] Axel Antoine, Sylvain Malacria, and Géry Casiez. 2017. ForceEdge: Controlling Autoscroll on Both Desktop and Mobile Computers Using the Force. In *Proceedings of the 2017 CHI Conference on Human Factors in Computing Systems* (Denver, Colorado, USA) *(CHI '17)*. Association for Computing Machinery, New York, NY, USA, 3281–3292. doi:10.1145/3025453.3025605

[4] Madeline Balaam, Anna Ståhl, Guðrún Margrét Ívansdóttir, Hallbjörg Embla Sigtryggsdóttir, Kristina Höök, and Caroline Yan Zheng. 2024. Exploring the Somatic Possibilities of Shape Changing Car Seats. In *Proceedings of the 2024 ACM Designing Interactive Systems Conference* (Copenhagen, Denmark) *(DIS '24)*. Association for Computing Machinery, New York, NY, USA, 3354–3371. doi:10.1145/3643834.3661518

[5] Gareth Barnaby and Anne Roudaut. 2019. Mantis: A Scalable, Lightweight and Accessible Architecture to Build Multiform Force Feedback Systems. In *Proceedings of the 32nd Annual ACM Symposium on User Interface Software and Technology* (New Orleans, LA, USA) *(UIST '19)*. Association for Computing Machinery, New York, NY, USA, 937–948. doi:10.1145/3332165.3347909

[6] Scott Bezek. 2022. SmartKnob. https://github.com/scottbez1/smartknob. Accessed: 2025-07-14.

[7] Alberto Boem and Giovanni Maria Troiano. 2019. Non-Rigid HCI: A Review of Deformable Interfaces and Input. In *Proceedings of the 2019 on Designing Interactive Systems Conference (DIS '19)*. Association for Computing Machinery, New York, NY, USA, 885–906. doi:10.1145/3322276.3322347

[8] Stephen Brewster and Lorna M. Brown. 2004. Tactons: structured tactile messages for non-visual information display. In *Proceedings of the Fifth Conference on Australasian User Interface - Volume 28* (Dunedin, New Zealand) *(AUIC '04)*. Australian Computer Society, Inc., AUS, 15–23.

[9] Michael Chamunorwa, Mikołaj P. Wozniak, Sarah Vöge, Heiko Müller, and Susanne C.J. Boll. 2022. Interacting with Rigid and Soft Surfaces for Smart-Home Control. *Proc. ACM Hum.-Comput. Interact.* 6, MHCI, Article 211 (sep 2022), 22 pages. doi:10.1145/3546746

[10] Yanjun Chen, Xuewei Liang, Si Chen, Yuwen Chen, Hongnan Lin, Hechuan Zhang, Chutian Jiang, Feng Tian, Yu Zhang, Shanshan Yao, and Teng Han. 2022. HapTag: A Compact Actuator for Rendering Push-Button Tactility on Soft Surfaces. In *Proceedings of the 35th Annual ACM Symposium on User Interface Software and Technology* (Bend, OR, USA) *(UIST '22)*. Association for Computing Machinery, New York, NY, USA, Article 70, 11 pages. doi:10.1145/3526113.3545644

[11] Kyung Yun Choi, Jinmo Lee, Neska ElHaouij, Rosalind Picard, and Hiroshi Ishii. 2021. aSpire: Clippable, Mobile Pneumatic-Haptic Device for Breathing Rate Regulation via Personalizable Tactile Feedback. In *Extended Abstracts of the 2021 CHI Conference on Human Factors in Computing Systems* (Yokohama, Japan) *(CHI EA '21)*. Association for Computing Machinery, New York, NY, USA, Article 372, 8 pages. doi:10.1145/3411763.3451602

[12] Christian Corsten, Simon Voelker, Andreas Link, and Jan Borchers. 2018. Use the Force Picker, Luke: Space-Efficient Value Input on Force-Sensitive Mobile Touchscreens. In *Proceedings of the 2018 CHI Conference on Human Factors in Computing Systems*. ACM, Montreal QC Canada, 1–12. doi:10.1145/3173574.3174235

[13] Martin Culjat, Chih-Hung King, Miguel Franco, James Bisley, Warren Grundfest, and Erik Dutson. 2008. Pneumatic balloon actuators for tactile feedback in robotic surgery. *Industrial Robot: An International Journal* 35, 5 (2008), 449–455.

[14] Alexandra Delazio, Ken Nakagaki, Roberta L. Klatzky, Scott E. Hudson, Jill Fain Lehman, and Alanson P. Sample. 2018. Force Jacket: Pneumatically-Actuated Jacket for Embodied Haptic Experiences. In *Proceedings of the 2018 CHI Conference on Human Factors in Computing Systems* (Montreal QC, Canada) *(CHI '18)*. Association for Computing Machinery, New York, NY, USA, 1–12. doi:10.1145/3173574.3173894

[15] Yifan Fan, Nico Pietroni, and Sam Ferguson. 2023. A Neural Network-based Low-cost Soft Sensor for Touch Recognition and Deformation Capture. In *Proceedings of the 2023 ACM Designing Interactive Systems Conference* (Pittsburgh, PA, USA) *(DIS '23)*. Association for Computing Machinery, New York, NY, USA, 889–903. doi:10.1145/3563657.3595963

[16] Elias Fares, Victor Cheung, and Audrey Girouard. 2017. Effects of Bend Gesture Training on Learnability and Memorability in a Mobile Game. In *Proceedings of the 2017 ACM International Conference on Interactive Surfaces and Spaces* (Brighton, United Kingdom) *(ISS '17)*. Association for Computing Machinery, New York, NY, USA, 240–245. doi:10.1145/3132272.3134142

[17] Alexz Farrall, Jordan Taylor, Ben Ainsworth, and Jason Alexander. 2023. Manifesting Breath: Empirical Evidence for the Integration of Shape-changing Biofeedback-based Artefacts within Digital Mental Health Interventions. In *Proceedings of the 2023 CHI Conference on Human Factors in Computing Systems* (Hamburg, Germany) *(CHI '23)*. Association for Computing Machinery, New York, NY, USA, Article 497, 14 pages. doi:10.1145/3544548.3581188

[18] Amir Firouzeh, Ayana Mizutani, Jonas Groten, Martin Zirkl, and Herbert Shea. 2024. PopTouch: A Submillimeter Thick Dynamically Reconfigured Haptic Interface with Pressable Buttons. *Advanced Materials* 36, 8 (2024), 2307636. arXiv:https://advanced.onlinelibrary.wiley.com/doi/pdf/10.1002/adma.202307636 doi:10.1002/adma.202307636

[19] Sean Follmer, Daniel Leithinger, Alex Olwal, Nadia Cheng, and Hiroshi Ishii. 2012. Jamming User Interfaces: Programmable Particle Stiffness and Sensing for Malleable and Shape-changing Devices. In *Proceedings of the 25th Annual ACM Symposium on User Interface Software and Technology (UIST '12)*. ACM, New York, NY, USA, 519–528. doi:10.1145/2380116.2380181

[20] Sean Follmer, Daniel Leithinger, Alex Olwal, Akimitsu Hogge, and Hiroshi Ishii. 2013. inFORM: Dynamic Physical Affordances and Constraints Through Shape and Object Actuation. In *Proceedings of the 26th Annual ACM Symposium on User Interface Software and Technology (UIST '13)*. ACM, New York, NY, USA,

417–426. doi:10.1145/2501988.2502032

[21] Marcus Friedel, Ehud Sharlin, and Ryo Suzuki. 2022. HapticLever: Kinematic Force Feedback using a 3D Pantograph. In *Adjunct Proceedings of the 35th Annual ACM Symposium on User Interface Software and Technology* (Bend, OR, USA) *(UIST '22 Adjunct)*. Association for Computing Machinery, New York, NY, USA, Article 47, 4 pages. doi:10.1145/3526114.3558736

[22] Bruno Fruchard, Paul Strohmeier, Roland Bennewitz, and Jürgen Steimle. 2021. Squish This: Force Input on Soft Surfaces for Visual Targeting Tasks. In *Proceedings of the 2021 CHI Conference on Human Factors in Computing Systems* (Yokohama, Japan) *(CHI '21)*. Association for Computing Machinery, New York, NY, USA, Article 219, 9 pages. doi:10.1145/3411764.3445623

[23] Juri Fujii, Satoshi Nakamaru, and Yasuaki Kakehi. 2021. LayerPump: Rapid Prototyping of Functional 3D Objects with Built-in Electrohydrodynamics Pumps Based on Layered Plates. In *Proceedings of the Fifteenth International Conference on Tangible, Embedded, and Embodied Interaction* (Salzburg, Austria) *(TEI '21)*. Association for Computing Machinery, New York, NY, USA, Article 48, 7 pages. doi:10.1145/3430524.3442453

[24] Audrey Girouard, Jessica Lo, Md Riyadh, Farshad Daliri, Alexander Keith Eady, and Jerome Pasquero. 2015. One-Handed Bend Interactions with Deformable Smartphones. In *Proceedings of the 33rd Annual ACM Conference on Human Factors in Computing Systems* (Seoul, Republic of Korea) *(CHI '15)*. Association for Computing Machinery, New York, NY, USA, 1509–1518. doi:10.1145/2702123.2702513

[25] Kristian Gohlke, Wolfgang Sattler, and Eva Hornecker. 2022. AirPinch – An Inflatable Touch Fader with Pneumatic Tactile Feedback. In *Proceedings of the Sixteenth International Conference on Tangible, Embedded, and Embodied Interaction* (Daejeon, Republic of Korea) *(TEI '22)*. Association for Computing Machinery, New York, NY, USA, Article 64, 6 pages. doi:10.1145/3490149.3505568

[26] Jesse T Gonzalez and Scott E Hudson. 2022. Layer by Layer, Patterned Valves Enable Programmable Soft Surfaces. *Proceedings of the ACM on Interactive, Mobile, Wearable and Ubiquitous Technologies* 6, 1 (2022), 1–25.

[27] Maas Goudswaard, Abel Abraham, Bruna Goveia da Rocha, Kristina Andersen, and Rong-Hao Liang. 2020. FabriClick: Interweaving Pushbuttons into Fabrics Using 3D Printing and Digital Embroidery. In *Proceedings of the 2020 ACM Designing Interactive Systems Conference* (Eindhoven, Netherlands) *(DIS '20)*. Association for Computing Machinery, New York, NY, USA, 379–393. doi:10.1145/3357236.3395569

[28] Jaehyun Han, Seongkook Heo, Jiseong Gu, and Geehyuk Lee. 2014. Trampoline: A Double-Sided Elastic Touch Device for Repoussé and Chasing Techniques. In *CHI '14 Extended Abstracts on Human Factors in Computing Systems*. ACM, Toronto Ontario Canada, 1627–1632. doi:10.1145/2559206.2581252

[29] Teng Han, Fraser Anderson, Pourang Irani, and Tovi Grossman. 2018. HydroRing: Supporting Mixed Reality Haptics Using Liquid Flow. In *Proceedings of the 31st Annual ACM Symposium on User Interface Software and Technology* (Berlin, Germany) *(UIST '18)*. Association for Computing Machinery, New York, NY, USA, 913–925. doi:10.1145/3242587.3242667

[30] Teng Han, Qian Han, Michelle Annett, Fraser Anderson, Da-Yuan Huang, and Xing-Dong Yang. 2017. Frictio: Passive Kinesthetic Force Feedback for Smart Ring Output. In *Proceedings of the 30th Annual ACM Symposium on User Interface Software and Technology* (Québec City, QC, Canada) *(UIST '17)*. Association for Computing Machinery, New York, NY, USA, 131–142. doi:10.1145/3126594.3126622

[31] Liang He, Gierad Laput, Eric Brockmeyer, and Jon E. Froehlich. 2017. SqueezaPulse: Adding Interactive Input to Fabricated Objects Using Corrugated Tubes and Air Pulses. In *Proceedings of the Eleventh International Conference on Tangible, Embedded, and Embodied Interaction (TEI '17)*. ACM, New York, NY, USA, 341–350. doi:10.1145/3024969.3024976

[32] Jonas Hepp and Alexander Badri-Spröwitz. 2022. A Novel Spider-Inspired Rotary-Rolling Diaphragm Actuator with Linear Torque Characteristic and High Mechanical Efficiency. *Soft Robotics* 9, 2 (2022), 364–375. arXiv:https://doi.org/10.1089/soro.2020.0108 doi:10.1089/soro.2020.0108 PMID: 34166108.

[33] Gero Herkenrath, Thorsten Karrer, and Jan Borchers. 2008. Twend: twisting and bending as new interaction gesture in mobile devices. In *CHI '08 Extended Abstracts on Human Factors in Computing Systems* (Florence, Italy) *(CHI EA '08)*. Association for Computing Machinery, New York, NY, USA, 3819–3824. doi:10.1145/1358628.1358936

[34] Peter Keith Brian Hodges. 1996. 23 - Health and Safety. In *Hydraulic Fluids*, Peter Keith Brian Hodges (Ed.). Butterworth-Heinemann, London, 153–155. doi:10.1016/B978-034067652-3/50024-5

[35] Yvonne Jansen, Thorsten Karrer, and Jan Borchers. 2010. MudPad: A Tactile Memory Game. In *ACM International Conference on Interactive Tabletops and Surfaces (ITS '10)*. ACM, New York, NY, USA, 306–306. doi:10.1145/1936652.1936734

[36] Yvonne Jansen, Thorsten Karrer, and Jan Borchers. 2010. MudPad: Tactile Feedback and Haptic Texture Overlay for Touch Surfaces. In *ACM International Conference on Interactive Tabletops and Surfaces (ITS '10)*. ACM, New York, NY, USA, 11–14. doi:10.1145/1936652.1936655

[37] Arata Jingu, Nihar Sabnis, Paul Strohmeier, and Jürgen Steimle. 2024. Shaping Compliance: Inducing Haptic Illusion of Compliance in Different Shapes with Electrotactile Grains. In *Proceedings of the CHI Conference on Human Factors in Computing Systems* (Honolulu, HI, USA) *(CHI '24)*. Association for Computing Machinery, New York, NY, USA, Article 432, 13 pages. doi:10.1145/3613904.3641907

[38] Romina Kettner, Patrick Bader, Thomas Kosch, Stefan Schneegass, and Albrecht Schmidt. 2017. Towards pressure-based feedback for non-stressful tactile notifications. In *Proceedings of the 19th International Conference on Human-Computer Interaction with Mobile Devices and Services* (Vienna, Austria) *(MobileHCI '17)*. Association for Computing Machinery, New York, NY, USA, Article 89, 8 pages. doi:10.1145/3098279.3122132

[39] Johan Kildal, Andrés Lucero, and Marion Boberg. 2013. Twisting touch: combining deformation and touch as input within the same interaction cycle on handheld devices. In *Proceedings of the 15th International Conference on Human-Computer Interaction with Mobile Devices and Services* (Munich, Germany) *(MobileHCI '13)*. Association for Computing Machinery, New York, NY, USA, 237–246. doi:10.1145/2493190.2493238

[40] Hyunyoung Kim, Céline Coutrix, and Anne Roudaut. 2016. KnobSlider: Design of a Shape-changing Device Grounded in Users' Needs. In *Actes De La 28IÈMe ConfÉRence Francophone Sur L'Interaction Homme-Machine (IHM '16)*. ACM, New York, NY, USA, 91–102. doi:10.1145/3004107.3004125

[41] Seoktae Kim, Hyunjung Kim, Boram Lee, Tek-Jin Nam, and Woohun Lee. 2008. Inflatable Mouse: Volume-adjustable Mouse with Air-pressure-sensitive Input and Haptic Feedback. In *Proceedings of the SIGCHI Conference on Human Factors in Computing Systems (CHI '08)*. ACM, New York, NY, USA, 211–224. doi:10.1145/1357054.1357090

[42] David Ledo, Steven Houben, Jo Vermeulen, Nicolai Marquardt, Lora Oehlberg, and Saul Greenberg. 2018. Evaluation Strategies for HCI Toolkit Research. In *Proceedings of the 2018 CHI Conference on Human Factors in Computing Systems* (Montreal QC, Canada) *(CHI '18)*. Association for Computing Machinery, New York, NY, USA, 1–17. doi:10.1145/3173574.3173610

[43] Hyowon Lee, Andrew Cheah Huei Yoong, Simon Lui, Anuroop Vaniyar, and Gayathri Balasubramanian. 2016. Design exploration for the "squeezable" interaction. In *Proceedings of the 28th Australian Conference on Computer-Human Interaction* (Launceston, Tasmania, Australia) *(OzCHI '16)*. Association for Computing Machinery, New York, NY, USA, 586–594. doi:10.1145/3010915.3010930

[44] Sang-Su Lee, Sohyun Kim, Bopil Jin, Eunji Choi, Boa Kim, Xu Jia, Daeeop Kim, and Kun-pyo Lee. 2010. How users manipulate deformable displays as input devices. In *Proceedings of the SIGCHI Conference on Human Factors in Computing Systems* (Atlanta, Georgia, USA) *(CHI '10)*. Association for Computing Machinery, New York, NY, USA, 1647–1656. doi:10.1145/1753326.1753572

[45] Yi-Chi Liao, Sunjun Kim, Byungjoo Lee, and Antti Oulasvirta. 2020. Button Simulation and Design via FDVV Models. In *Proceedings of the 2020 CHI Conference on Human Factors in Computing Systems*. Association for Computing Machinery, New York, NY, USA, 1–14.

[46] Yi-Chi Liao, Sunjun Kim, and Antti Oulasvirta. 2018. One Button to Rule Them All: Rendering Arbitrary Force-Displacement Curves. In *The 31st Annual ACM Symposium on User Interface Software and Technology Adjunct Proceedings (UIST '18 Adjunct)*. Association for Computing Machinery, New York, NY, USA, 111–113. doi:10.1145/3266037.3266118

[47] Hongnan Lin, Liang He, Fangli Song, Yifan Li, Tingyu Cheng, Clement Zheng, Wei Wang, and HyunJoo Oh. 2022. FlexHaptics: A Design Method for Passive Haptic Inputs Using Planar Compliant Structures. In *Proceedings of the 2022 CHI Conference on Human Factors in Computing Systems* (New Orleans, LA, USA) *(CHI '22)*. Association for Computing Machinery, New York, NY, USA, Article 169, 13 pages. doi:10.1145/3491102.3502113

[48] Qiuyu Lu, Jifei Ou, Lining Yao, and Hiroshi Ishii. 2024. milleCrepe: Extending Capabilities of Fluid-driven Interfaces with Multilayer Structures and Diverse Actuation Media. In *Extended Abstracts of the CHI Conference on Human Factors in Computing Systems* (Honolulu, HI, USA) *(CHI EA '24)*. Association for Computing Machinery, New York, NY, USA, Article 383, 10 pages. doi:10.1145/3613905.3650891

[49] Robert MacCurdy, Robert Katzschmann, Youbin Kim, and Daniela Rus. 2016. Printable hydraulics: A method for fabricating robots by 3D co-printing solids and liquids. In *2016 IEEE International Conference on Robotics and Automation (ICRA)* (Stockholm, Sweden). IEEE Press, 3878–3885. doi:10.1109/ICRA.2016.7487576

[50] Justin Matejka, Michael Glueck, Erin Bradner, Ali Hashemi, Tovi Grossman, and George Fitzmaurice. 2018. Dream Lens: Exploration and Visualization of Large-Scale Generative Design Datasets. In *Proceedings of the 2018 CHI Conference on Human Factors in Computing Systems* (Montreal QC, Canada) *(CHI '18)*. Association for Computing Machinery, New York, NY, USA, 1–12. doi:10.1145/3173574.3173943

[51] Mustafa Mete, Haewon Jeong, Wei Dawid Wang, and Jamie Paik. 2024. SORI: A softness-rendering interface to unravel the nature of softness perception. *Proceedings of the National Academy of Sciences* 121, 13 (2024), e2314901121.

arXiv:https://www.pnas.org/doi/pdf/10.1073/pnas.2314901121 doi:10.1073/pnas.2314901121

[52] Viktor Miruchna, Robert Walter, David Lindlbauer, Maren Lehmann, Regine von Klitzing, and Jorg Muller. 2015. GelTouch: Localized Tactile Feedback Through Thin, Programmable Gel. In *Proceedings of the 28th Annual ACM Symposium on User Interface Software & Technology (UIST '15)*. ACM, New York, NY, USA, 3–10. doi:10.1145/2807442.2807487

[53] Geoffrey C. Morris, Sasha Leitman, and Marina Kassianidou. 2004. SillyTone Squish Factory. In *Proceedings of the 2004 Conference on New Interfaces for Musical Expression* (Hamamatsu, Shizuoka, Japan) *(NIME '04)*. National University of Singapore, SGP, 201–202.

[54] Ken Nakagaki, Daniel Fitzgerald, Zhiyao (John) Ma, Luke Vink, Daniel Levine, and Hiroshi Ishii. 2019. inFORCE: Bi-directional 'Force' Shape Display for Haptic Interaction. In *Proceedings of the Thirteenth International Conference on Tangible, Embedded, and Embodied Interaction (TEI '19)*. Association for Computing Machinery, New York, NY, USA, 615–623. doi:10.1145/3294109.3295621

[55] Shinichi Nakagawa and Holger Schielzeth. 2013. A general and simple method for obtaining R2 from generalized linear mixed-effects models. *Methods in ecology and evolution* 4, 2 (2013), 133–142.

[56] Ryosuke Nakayama, Ryo Suzuki, Satoshi Nakamaru, Ryuma Niiyama, Yoshihiro Kawahara, and Yasuaki Kakehi. 2019. MorphIO: Entirely Soft Sensing and Actuation Modules for Programming Shape Changes through Tangible Interaction. In *Proceedings of the 2019 on Designing Interactive Systems Conference* (San Diego, CA, USA) *(DIS '19)*. Association for Computing Machinery, New York, NY, USA, 975–986. doi:10.1145/3322276.3322337

[57] James Nash, Kim Sauvé, Adwait Sharma, Christopher Clarke, and Jason Alexander. 2025. Investigating the Impact of Deformable, Movable, and Rigid Surfaces on Force-Input Interactions. *ACM Trans. Comput.-Hum. Interact.* (May 2025). doi:10.1145/3736409 Just Accepted.

[58] James Nash, Kim Sauvé, Anke van Oosterhout, Catharina Maria van Riet, Adwait Sharma, Christopher Clarke, and Jason Alexander. 2024. Feelix HydroHaptics. https://github.com/ankevanoosterhout/Feelix_hydrohaptics. Accessed: 2025-07-14.

[59] James David Nash, Cameron Steer, Teodora Dinca, Adwait Sharma, Alvaro Favaratto Santos, Benjamin Timothy Wildgoose, Alexander Ager, Christopher Clarke, and Jason Alexander. 2024. DeformIO: Dynamic Stiffness Control on a Deformable Force-sensing Display. In *Extended Abstracts of the 2024 CHI Conference on Human Factors in Computing Systems* (Honolulu, HI, USA) *(CHI EA '24)*. Association for Computing Machinery, New York, NY, USA, Article 98, 8 pages. doi:10.1145/3613905.3650772

[60] Alex Olwal, Jon Moeller, Greg Priest-Dorman, Thad Starner, and Ben Carroll. 2018. I/O Braid: Scalable Touch-Sensitive Lighted Cords Using Spiraling, Repeating Sensing Textiles and Fiber Optics. In *Proceedings of the 31st Annual ACM Symposium on User Interface Software and Technology* (Berlin, Germany) *(UIST '18)*. Association for Computing Machinery, New York, NY, USA, 485–497. doi:10.1145/3242587.3242638

[61] Jifei Ou, Felix Heibeck, and Hiroshi Ishii. 2016. TEI 2016 Studio: Inflated Curiosity. In *Proceedings of the TEI '16: Tenth International Conference on Tangible, Embedded, and Embodied Interaction* (Eindhoven, Netherlands) *(TEI '16)*. Association for Computing Machinery, New York, NY, USA, 766–769. doi:10.1145/2839462.2854119

[62] Amanda Parkes, Vincent LeClerc, and Hiroshi Ishii. 2006. Glume: exploring materiality in a soft augmented modular modeling system. In *CHI '06 Extended Abstracts on Human Factors in Computing Systems* (Montréal, Québec, Canada) *(CHI EA '06)*. Association for Computing Machinery, New York, NY, USA, 1211–1216. doi:10.1145/1125451.1125678

[63] Patrick Parzer, Adwait Sharma, Anita Vogl, Jürgen Steimle, Alex Olwal, and Michael Haller. 2017. SmartSleeve: Real-time Sensing of Surface and Deformation Gestures on Flexible, Interactive Textiles, using a Hybrid Gesture Detection Pipeline. In *Proceedings of the 30th Annual ACM Symposium on User Interface Software and Technology* (Québec City, QC, Canada) *(UIST '17)*. Association for Computing Machinery, New York, NY, USA, 565–577. doi:10.1145/3126594.3126652

[64] F. Pedregosa, G. Varoquaux, A. Gramfort, V. Michel, B. Thirion, O. Grisel, M. Blondel, P. Prettenhofer, R. Weiss, V. Dubourg, J. Vanderplas, A. Passos, D. Cournapeau, M. Brucher, M. Perrot, and E. Duchesnay. 2011. Scikit-learn: Machine Learning in Python. *Journal of Machine Learning Research* 12 (2011), 2825–2830.

[65] Henning Pohl, Peter Brandes, Hung Ngo Quang, and Michael Rohs. 2017. Squeezeback: Pneumatic Compression for Notifications. In *Proceedings of the 2017 CHI Conference on Human Factors in Computing Systems* (Denver, Colorado, USA) *(CHI '17)*. Association for Computing Machinery, New York, NY, USA, 5318–5330. doi:10.1145/3025453.3025526

[66] Tucker Rae-Grant, Chris Harrison, and Craig Shultz. 2024. DynaButtons: Fast Interactive Soft Buttons with Analog Control. In *2024 IEEE Haptics Symposium (HAPTICS)*. 366–371. doi:10.1109/HAPTICS59260.2024.10520864

[67] Lukas Rambold, Robert Kovacs, Conrad Lempert, Muhammad Abdullah, Helena Lendowski, Lukas Fritzsche, Martin Taraz, and Patrick Baudisch. 2023. AirTied: Automatic Personal Fabrication of Truss Structures. In *Proceedings of the 36th Annual ACM Symposium on User Interface Software and Technology* (San Francisco, CA, USA) *(UIST '23)*. Association for Computing Machinery, New York, NY, USA, Article 57, 10 pages. doi:10.1145/3586183.3606820

[68] Olivia G Ruston, Adwait Sharma, and Mike Fraser. 2024. SeamSleeve: Robust Arm Movement Sensing through Powered Stitching. In *Proceedings of the 2024 ACM Designing Interactive Systems Conference* (Copenhagen, Denmark) *(DIS '24)*. Association for Computing Machinery, New York, NY, USA, 1134–1147. doi:10.1145/3643834.3660726

[69] Rei Sakura, Changyo Han, Yahui Lyu, Keisuke Watanabe, Ryosuke Yamamura, and Yasuaki Kakehi. 2023. LattiSense: A 3D-Printable Resistive Deformation Sensor with Lattice Structures. In *Proceedings of the 8th ACM Symposium on Computational Fabrication* (New York City, NY, USA) *(SCF '23)*. Association for Computing Machinery, New York, NY, USA, Article 2, 14 pages. doi:10.1145/3623263.3623361

[70] Harpreet Sareen, Udayan Umapathi, Patrick Shin, Yasuaki Kakehi, Jifei Ou, Hiroshi Ishii, and Pattie Maes. 2017. Printflatables: Printing Human-Scale, Functional and Dynamic Inflatable Objects. In *Proceedings of the 2017 CHI Conference on Human Factors in Computing Systems* (Denver, Colorado, USA) *(CHI '17)*. Association for Computing Machinery, New York, NY, USA, 3669–3680. doi:10.1145/3025453.3025898

[71] Martin Schmitz, Jürgen Steimle, Jochen Huber, Niloofar Dezfuli, and Max Mühlhäuser. 2017. Flexibles: Deformation-Aware 3D-Printed Tangibles for Capacitive Touchscreens. In *Proceedings of the 2017 CHI Conference on Human Factors in Computing Systems* (Denver, Colorado, USA) *(CHI '17)*. Association for Computing Machinery, New York, NY, USA, 1001–1014. doi:10.1145/3025453.3025663

[72] Vivian Shen, Tucker Rae-Grant, Joe Mullenbach, Chris Harrison, and Craig Shultz. 2023. Fluid Reality: High-Resolution, Untethered Haptic Gloves using Electroosmotic Pump Arrays. In *Proceedings of the 36th Annual ACM Symposium on User Interface Software and Technology* (San Francisco, CA, USA) *(UIST '23)*. Association for Computing Machinery, New York, NY, USA, Article 8, 20 pages. doi:10.1145/3586183.3606771

[73] Craig Shultz and Chris Harrison. 2023. Flat Panel Haptics: Embedded Electroosmotic Pumps for Scalable Shape Displays. In *Proceedings of the 2023 CHI Conference on Human Factors in Computing Systems* (Hamburg, Germany) *(CHI '23)*. Association for Computing Machinery, New York, NY, USA, Article 745, 16 pages. doi:10.1145/3544548.3581547

[74] Mike Sinclair, Michel Pahud, and Hrvoje Benko. 2014. TouchMover 2.0 - 3D touchscreen with force feedback and haptic texture. In *2014 IEEE Haptics Symposium (HAPTICS)*. Institute of Electrical and Electronics Engineers, Houston, Tx, USA, 1–6. doi:10.1109/HAPTICS.2014.6775425

[75] Antun Skuric, Hasan Sinan Bank, Richard Unger, Owen Williams, and David González-Reyes. 2022. SimpleFOC: A Field Oriented Control (FOC) Library for Controlling Brushless Direct Current (BLDC) and Stepper Motors. *Journal of Open Source Software* 7, 74 (2022), 4232. doi:10.21105/joss.04232

[76] Ronit Slyper and Jessica Hodgins. 2012. Prototyping robot appearance, movement, and interactions using flexible 3D printing and air pressure sensors. In *2012 IEEE RO-MAN: The 21st IEEE International Symposium on Robot and Human Interactive Communication*. 6–11. doi:10.1109/ROMAN.2012.6343723

[77] M. A. Srinivasan and R. H. LaMotte. 1995. Tactual Discrimination of Softness. *Journal of Neurophysiology* 73, 1 (Jan. 1995), 88–101. doi:10.1152/jn.1995.73.1.88

[78] Andrew A. Stanley, James C. Gwilliam, and Allison M. Okamura. 2013. Haptic Jamming: A Deformable Geometry, Variable Stiffness Tactile Display Using Pneumatics and Particle Jamming. In *2013 World Haptics Conference (WHC)*. IEEE Computer Society, Washington, DC, USA, 25–30. doi:10.1109/WHC.2013.6548379

[79] Gianni Stano, Luca Arleo, and Gianluca Percoco. 2020. Additive Manufacturing for Soft Robotics: Design and Fabrication of Airtight, Monolithic Bending PneuNets with Embedded Air Connectors. *Micromachines* 11, 5 (2020). doi:10.3390/mi11050485

[80] Cameron Steer, Teodora Dinca, Crescent Jicol, Michael J Proulx, and Jason Alexander. 2023. Feel the Force, See the Force: Exploring Visual-tactile Associations of Deformable Surfaces with Colours and Shapes. In *Proceedings of the 2023 CHI Conference on Human Factors in Computing Systems* (Hamburg, Germany) *(CHI '23)*. Association for Computing Machinery, New York, NY, USA, Article 261, 13 pages. doi:10.1145/3544548.3580830

[81] Cameron Steer, Jennifer Pearson, Simon Robinson, and Matt Jones. 2017. Deformable Paint Palette: Actuated Force Controls for Digital Painting. In *Proceedings of the 2017 CHI Conference Extended Abstracts on Human Factors in Computing Systems (CHI EA '17)*. ACM, New York, NY, USA, 2936–2943. doi:10.1145/3027063.3053219

[82] Cameron Steer, Kim Sauvé, Anika Jain, Omosunmisola Lawal, Michael J Proulx, Crescent Jicol, and Jason Alexander. 2024. Squishy, Yet Satisfying: Exploring Deformable Shapes' Cross-Modal Correspondences with Colours and Emotions. In *Proceedings of the CHI Conference on Human Factors in Computing Systems* (Honolulu, HI, USA) *(CHI '24)*. Association for Computing Machinery, New York, NY, USA, Article 331, 20 pages. doi:10.1145/3613904.3641952

[83] Carolin Stellmacher, Feri Irsanto Pujianto, Tanja Kojic, Jan-Niklas Voigt-Antons, and Johannes Schöning. 2024. Experiencing Dynamic Weight Changes in Virtual Reality Through Pseudo-Haptics and Vibrotactile Feedback. In *Proceedings of the CHI Conference on Human Factors in Computing Systems* (Honolulu, HI, USA) *(CHI '24)*. Association for Computing Machinery, New York, NY, USA, Article 421, 13 pages. doi:10.1145/3613904.3642552

[84] Evgeny Stemasov, Simon Demharter, Max Rädler, Jan Gugenheimer, and Enrico Rukzio. 2024. pARam: Leveraging Parametric Design in Extended Reality to Support the Personalization of Artifacts for Personal Fabrication. In *Proceedings of the 2024 CHI Conference on Human Factors in Computing Systems* (Honolulu, HI, USA) *(CHI '24)*. Association for Computing Machinery, New York, NY, USA, Article 337, 22 pages. doi:10.1145/3613904.3642083

[85] Andrew Stevenson, Christopher Perez, and Roel Vertegaal. 2010. An Inflatable Hemispherical Multi-Touch Display. In *Proceedings of the Fifth International Conference on Tangible, Embedded, and Embodied Interaction* (Funchal, Portugal) *(TEI '11)*. Association for Computing Machinery, New York, NY, USA, 289–292. doi:10.1145/1935701.1935766

[86] Martin A. Stoffel, Shinichi Nakagawa, and Holger Schielzeth. 2021. `partR2`: partitioning R^2 in generalized linear mixed models. *PeerJ* 9 (May 2021), e11414. doi:10.7717/peerj.11414

[87] Tim Claudius Stratmann, Shadan Sadeghian Borojeni, Wilko Heuten, and Susanne C.J. Boll. 2018. ShoulderTap - Pneumatic On-body Cues to Encode Directions. In *Extended Abstracts of the 2018 CHI Conference on Human Factors in Computing Systems* (Montreal QC, Canada) *(CHI EA '18)*. Association for Computing Machinery, New York, NY, USA, 1–6. doi:10.1145/3170427.3188624

[88] Faisal Taher, John Vidler, and Jason Alexander. 2017. A Characterization of Actuation Techniques for Generating Movement in Shape-Changing Interfaces. *International Journal of Human–Computer Interaction* 33, 5 (2017), 385–398. doi:10.1080/10447318.2016.1250372

[89] Mark Thielen, Rohan Joshi, Frank Delbressine, Sidarto Bambang Oetomo, and Loe Feijs. 2017. An innovative design for cardiopulmonary resuscitation manikins based on a human-like thorax and embedded flow sensors. *Proceedings of the Institution of Mechanical Engineers, Part H* 231, 3 (2017), 243–249. arXiv:https://doi.org/10.1177/0954411917691555 doi:10.1177/0954411917691555 PMID: 28290239.

[90] Giovanni Maria Troiano, Esben Warming Pedersen, and Kasper Hornbæk. 2014. User-defined gestures for elastic, deformable displays. In *Proceedings of the 2014 International Working Conference on Advanced Visual Interfaces* (Como, Italy) *(AVI '14)*. Association for Computing Machinery, New York, NY, USA, 1–8. doi:10.1145/2598153.2598184

[91] Jessica Tsimeris, Duncan Stevenson, Tom Gedeon, and Matt Adcock. 2013. Using ForceForm, a Dynamically Deformable Interactive Surface, for Palpation Simulation in Medical Scenarios. In *Proceedings of the Second International Workshop on Smart Material Interfaces: Another Step to a Material Future (SMI '13)*. ACM, New York, NY, USA, 19–22. doi:10.1145/2534688.2534693

[92] Juliette S. van Haren, Katie Verschueren, Frank L.M. Delbressine, Merijn Beijes, and Catharina M. van Riet. 2024. Development and assessment of a cyanosis simulator in a fetal manikin for extra-uterine life support innovation. In *Proceedings of the 2023 10th International Conference on Biomedical and Bioinformatics Engineering* (Kyoto, Japan) *(ICBBE '23)*. Association for Computing Machinery, New York, NY, USA, 252–261. doi:10.1145/3637732.3637749

[93] Anke van Oosterhout. 2024. Feelix. https://github.com/ankevanoosterhout/Feelix. Accessed: 2025-07-14.

[94] Anke van Oosterhout, Miguel Bruns, and Eve Hoggan. 2020. Facilitating Flexible Force Feedback Design with Feelix. In *Proceedings of the 2020 International Conference on Multimodal Interaction (ICMI '20)*. Association for Computing Machinery, New York, NY, USA, 184–193. doi:10.1145/3382507.3418819

[95] Anke van Oosterhout, Miguel Bruns Alonso, and Satu Jumisko-Pyykkö. 2018. Ripple Thermostat: Affecting the Emotional Experience through Interactive Force Feedback and Shape Change. In *Proceedings of the 2018 CHI Conference on Human Factors in Computing Systems* (Montreal QC, Canada) *(CHI '18)*. Association for Computing Machinery, New York, NY, USA, 1–12. doi:10.1145/3173574.3174229

[96] Anke van Oosterhout and Eve Hoggan. 2021. Deformation Techniques for Shape Changing Interfaces. In *Extended Abstracts of the 2021 CHI Conference on Human Factors in Computing Systems* (Yokohama, Japan) *(CHI EA '21)*. Association for Computing Machinery, New York, NY, USA, Article 388, 7 pages. doi:10.1145/3411763.3451622

[97] Anke van Oosterhout, Eve Hoggan, Majken Kirkegaard Rasmussen, and Miguel Bruns. 2019. DynaKnob: Combining Haptic Force Feedback and Shape Change. In *Proceedings of the 2019 on Designing Interactive Systems Conference* (San Diego, CA, USA) *(DIS '19)*. Association for Computing Machinery, New York, NY, USA, 963–974. doi:10.1145/3322276.3322321

[98] Karen Vanderloock, Vero Vanden Abeele, Johan A.K. Suykens, and Luc Geurts. 2013. The skweezee system: enabling the design and the programming of squeeze interactions. In *Proceedings of the 26th Annual ACM Symposium on User Interface Software and Technology* (St. Andrews, Scotland, United Kingdom) *(UIST '13)*. Association for Computing Machinery, New York, NY, USA, 521–530. doi:10.1145/2501988.2502033

[99] Marynel Vázquez, Eric Brockmeyer, Ruta Desai, Chris Harrison, and Scott E. Hudson. 2015. 3D Printing Pneumatic Device Controls with Variable Activation Force Capabilities. In *Proceedings of the 33rd Annual ACM Conference on Human Factors in Computing Systems (CHI '15)*. ACM, New York, NY, USA, 1295–1304. doi:10.1145/2702123.2702569

[100] Feng Wang and Xiangshi Ren. 2009. Empirical evaluation for finger input properties in multi-touch interaction. In *Proceedings of the SIGCHI Conference on Human Factors in Computing Systems* (Boston, MA, USA) *(CHI '09)*. Association for Computing Machinery, New York, NY, USA, 1063–1072. doi:10.1145/1518701.1518864

[101] Yoshihiro Watanabe, Alvaro Cassinelli, Takashi Komuro, and Masatoshi Ishikawa. 2008. The deformable workspace: A membrane between real and virtual space. In *2008 3rd IEEE International Workshop on Horizontal Interactive Human Computer Systems*. IEEE Computer Society, Washington, DC, USA, 145–152. doi:10.1109/TABLETOP.2008.4660197

[102] Martin Weigel and Jürgen Steimle. 2017. DeformWear: Deformation Input on Tiny Wearable Devices. *Proc. ACM Interact. Mob. Wearable Ubiquitous Technol.* 1, 2, Article 28 (jun 2017), 23 pages. doi:10.1145/3090093

[103] Yannick Weiss, Steeven Villa, Albrecht Schmidt, Sven Mayer, and Florian Müller. 2023. Using Pseudo-Stiffness to Enrich the Haptic Experience in Virtual Reality. In *Proceedings of the 2023 CHI Conference on Human Factors in Computing Systems* (Hamburg,Germany) *(CHI '23)*. Association for Computing Machinery, New York, NY, USA, Article 388, 15 pages. doi:10.1145/3544548.3581223

[104] Eric W. Weisstein. 2025. Spherical Cap. From *MathWorld–A Wolfram Resource*. https://mathworld.wolfram.com/SphericalCap.html Accessed: 2025-07-14.

[105] Nicolaas Westerhof, Nikolaos Stergiopulos, Mark I. M. Noble, and Berend E. Westerhof. 2019. *Law of Poiseuille*. Springer International Publishing, Cham, 9–15. doi:10.1007/978-3-319-91932-4_2

[106] George M. Whitesides. 2018. Soft Robotics. *Angewandte Chemie International Edition* 57, 16 (2018), 4258–4273. arXiv:https://onlinelibrary.wiley.com/doi/pdf/10.1002/anie.201800907 doi:10.1002/anie.201800907

[107] John P. Whitney, Matthew F. Glisson, Eric L. Brockmeyer, and Jessica K. Hodgins. 2014. A low-friction passive fluid transmission and fluid-tendon soft actuator. In *2014 IEEE/RSJ International Conference on Intelligent Robots and Systems*. 2801–2808. doi:10.1109/IROS.2014.6942946

[108] Graham Wilson, Stephen A. Brewster, Martin Halvey, Andrew Crossan, and Craig Stewart. 2011. The Effects of Walking, Feedback and Control Method on Pressure-Based Interaction. In *Proceedings of the 13th International Conference on Human Computer Interaction with Mobile Devices and Services (MobileHCI '11)*. Association for Computing Machinery, New York, NY, USA, 147–156. doi:10.1145/2037373.2037397

[109] Songlin Xu, Zhiyuan Wu, Shunhong Wang, Rui Fan, and Nan Lin. 2020. Hydrauio: Extending Interaction Space on the Pen through Hydraulic Sensing and Haptic Output. In *Adjunct Proceedings of the 33rd Annual ACM Symposium on User Interface Software and Technology* (Virtual Event, USA) *(UIST '20 Adjunct)*. Association for Computing Machinery, New York, NY, USA, 43–45. doi:10.1145/3379350.3416180

[110] Zeyu Yan and Huaishu Peng. 2021. FabHydro: Printing Interactive Hydraulic Devices with an Affordable SLA 3D Printer. In *The 34th Annual ACM Symposium on User Interface Software and Technology* (Virtual Event, USA) *(UIST '21)*. Association for Computing Machinery, New York, NY, USA, 298–311. doi:10.1145/3472749.3474751

[111] Willa Yunqi Yang, Yifan Zou, Jingle Huang, Raouf Abujaber, and Ken Nakagaki. 2024. TorqueCapsules: Fully-Encapsulated Flywheel Actuation Modules for Designing and Prototyping Movement-Based and Kinesthetic Interaction. In *Proceedings of the 37th Annual ACM Symposium on User Interface Software and Technology* (Pittsburgh, PA, USA) *(UIST '24)*. Association for Computing Machinery, New York, NY, USA, Article 98, 15 pages. doi:10.1145/3654777.3676364

[112] Yue Yang, Lei Ren, Chuang Chen, Bin Hu, Zhuoyi Zhang, Xinyan Li, Yanchen Shen, Kuangqi Zhu, Junzhe Ji, Yuyang Zhang, Yongbo Ni, Jiayi Wu, Qi Wang, Jiang Wu, Lingyun Sun, Ye Tao, and Guanyun Wang. 2024. SnapInflatables: Designing Inflatables with Snap-through Instability for Responsive Interaction. In *Proceedings of the CHI Conference on Human Factors in Computing Systems* (Honolulu, HI, USA) *(CHI '24)*. Association for Computing Machinery, New York, NY, USA, Article 342, 15 pages. doi:10.1145/3613904.3642933

[113] Lining Yao, Ryuma Niiyama, Jifei Ou, Sean Follmer, Clark Della Silva, and Hiroshi Ishii. 2013. PneUI: pneumatically actuated soft composite materials for shape changing interfaces. In *Proceedings of the 26th Annual ACM Symposium on User Interface Software and Technology* (St. Andrews, Scotland, United Kingdom) *(UIST '13)*. Association for Computing Machinery, New York, NY, USA, 13–22. doi:10.1145/2501988.2502037

[114] Kentaro Yoshida, Hiroshi Suzuki, Hironobu Abe, Akira Ono, Hiroto Kawaguchi, Masahiro Sato, Yota Komoriya, and Kazunobu Ohkuri. 2021. Pneumatic Concave Deformable Device and Finger Deformation-Based Evaluation for Hardness

Perception. In *2021 IEEE World Haptics Conference (WHC)*. IEEE Computer Society, Montreal, Canada, 668–673. doi:10.1109/WHC49131.2021.9517139

[115] Jung-Hwan Youn, Seung Heon Lee, and Craig Shultz. 2025. HaptiCoil: Soft Programmable Buttons with Hydraulically Coupled Haptic Feedback and Sensing. In *Proceedings of the 2025 CHI Conference on Human Factors in Computing Systems (CHI '25)*. Association for Computing Machinery, New York, NY, USA, Article 155, 16 pages. doi:10.1145/3706598.3713175

[116] Yichen Zhai, Albert De Boer, Jiayao Yan, Benjamin Shih, Martin Faber, Joshua Speros, Rohini Gupta, and Michael T. Tolley. 2023. Desktop fabrication of monolithic soft robotic devices with embedded fluidic control circuits. *Science Robotics* 8, 79 (2023), eadg3792. arXiv:https://www.science.org/doi/pdf/10.1126/scirobotics.adg3792 doi:10.1126/scirobotics.adg3792

[117] Bowen Zhang and Misha Sra. 2021. PneuMod: A Modular Haptic Device with Localized Pressure and Thermal Feedback. In *Proceedings of the 27th ACM Symposium on Virtual Reality Software and Technology* (Osaka, Japan) *(VRST '21)*. Association for Computing Machinery, New York, NY, USA, Article 30, 7 pages. doi:10.1145/3489849.3489857

[118] Zhuoming Zhang, Jessalyn Alvina, Françoise Détienne, and Eric Lecolinet. 2022. Pulling, Pressing, and Sensing with In-Flat: Transparent Touch Overlay for Smartphones. In *Proceedings of the 2022 International Conference on Advanced Visual Interfaces* (Frascati, Rome, Italy) *(AVI 2022)*. Association for Computing Machinery, New York, NY, USA, Article 12, 9 pages. doi:10.1145/3531073.3531111

[119] Zining Zhang, Jiasheng Li, Zeyu Yan, Jun Nishida, and Huaishu Peng. 2024. JetUnit: Rendering Diverse Force Feedback in Virtual Reality Using Water Jets. In *Proceedings of the 37th Annual ACM Symposium on User Interface Software and Technology* (Pittsburgh, PA, USA) *(UIST '24)*. Association for Computing Machinery, New York, NY, USA, Article 136, 15 pages. doi:10.1145/3654777.3676440

[120] Clement Zheng, Zhen Zhou Yong, Hongnan Lin, HyunJoo Oh, and Ching Chiuan Yen. 2022. Shape-Haptics: Planar & Passive Force Feedback Mechanisms for Physical Interfaces. In *Proceedings of the 2022 CHI Conference on Human Factors in Computing Systems* (New Orleans, LA, USA) *(CHI '22)*. Association for Computing Machinery, New York, NY, USA, Article 171, 15 pages. doi:10.1145/3491102.3501829

[121] Mengjia Zhu, Amirhossein H. Memar, Aakar Gupta, Majed Samad, Priyanshu Agarwal, Yon Visell, Sean J. Keller, and Nicholas Colonnese. 2020. PneuSleeve: In-fabric Multimodal Actuation and Sensing in a Soft, Compact, and Expressive Haptic Sleeve. In *Proceedings of the 2020 CHI Conference on Human Factors in Computing Systems* (Honolulu, HI, USA) *(CHI '20)*. Association for Computing Machinery, New York, NY, USA, 1–12. doi:10.1145/3313831.3376333

A Additional results

Table 1: Pairwise post hoc comparisons of success rate for force feedback effects using estimated marginal means during the force feedback user study.

	Sample		df	Statistic	*p*	Effect Size
Line	**Factor 1**	**Factor 2**				
1	Boundary	Bumps	Inf	-2.65	.085	-0.74
2	Boundary	Button	Inf	-4.83	<.001	-1.51
3	Boundary	Click	Inf	-2.51	.120	-0.69
4	Boundary	Oscillating	Inf	-5.84	<.001	-2.08
5	Boundary	Stiffening	Inf	-4.01	.001	-1.19
6	Bumps	Button	Inf	-2.39	.158	-0.77
7	Bumps	Click	Inf	0.15	1.000	0.04
8	Bumps	Oscillating	Inf	-3.69	.003	-1.35
9	Bumps	Stiffening	Inf	-1.47	.683	-0.45
10	Button	Click	Inf	2.53	.115	0.81
11	Button	Oscillating	Inf	-1.48	.678	-0.57
12	Button	Stiffening	Inf	0.94	.935	0.32
13	Click	Oscillating	Inf	-3.82	.002	-1.39
14	Click	Stiffening	Inf	-1.61	.590	-0.49
15	Oscillating	Stiffening	Inf	2.36	.169	0.89